

Cosmology with Fast Radio Bursts

Marcin Glowacki^{a,b,c} and Khee-Gan Lee^{d,e}

^aInternational Centre for Radio Astronomy Research (ICRAR), Curtin University, Bentley, WA 6102, Australia

^bInstitute for Astronomy, University of Edinburgh, Royal Observatory, Edinburgh, EH9 3HJ, United Kingdom

^cInter-University Institute for Data Intensive Astronomy, Department of Astronomy, University of Cape Town, Cape Town, South Africa

^dKavli IPMU (WPI), UTIAS, The University of Tokyo, Kashiwa, Chiba 277-8583, Japan

^eCenter for Data Driven Discovery, Kavli IPMU (WPI), UTIAS, The University of Tokyo, Kashiwa, Chiba 277-8583, Japan

© 20xx Elsevier Ltd. All rights reserved.

First draft of Cosmology with Fast Radio Bursts for submission to the editors for Encyclopedia of Astrophysics 1st Edition.

Nomenclature

FRB	Fast radio burst
CGM	Circumgalactic medium
DM	Dispersion measure
Λ CDM	Λ Cold Dark Matter
CMB	Cosmic Microwave Background
BBN	Big Bang Nucleosynthesis
AGN	Active Galactic Nuclei
RM	Rotation measure
IGM	Intergalactic medium
IGrM	Intra-Group medium
ICM	Intra-cluster medium
H _I	Neutral hydrogen

Abstract

Despite the first detection of fast radio bursts (FRBs) being as recent as 2007, they have already been proven to be a fantastic tool as a unique cosmological probe. In this chapter, after a brief introduction to FRBs and how they are currently detected, we describe various cosmological questions and how FRB research has both aided previous studies and can continue to do so. Topics include placing constraints on cosmological parameters to understanding the distribution of baryons throughout the Universe. We conclude with some notes on the challenges to be overcome and best enable ongoing and future FRB-based studies of cosmology.

Learning Objectives

By the end of this chapter, you should understand:

- What are fast radio bursts (FRBs) and how they are found
- What dispersion measure is, its relation to ionized electrons, and how these electrons are distributed in the Universe
- How the Macquart relation was observed and continues to be studied
- How simulations can be combined with FRBs to probe the cosmic baryon distribution
- How FRBs can be used to constrain the Hubble constant, study cosmic magnetism, and address other cosmological questions
- The future steps for FRB research required to help solve cosmological mysteries

1 Fast radio bursts

Fast radio bursts (FRBs) are intense pulses of radio emission, having been observed at energies of $\sim 10^{38-43}$ erg. For perspective, while FRBs bear some resemblance to pulses from Galactic radio pulsars, their flux densities is some ten billion times larger. FRBs also crucially have not been seen to periodically repeat like pulsars. In fact, to date the majority of FRBs have only been detected once. A mere handful of FRBs to date have been seen to ‘repeat’ in an unpredictable manner hundreds to thousands of times, and only a few have exhibited identifiable activity windows to date. Remarkably, such intense emission from FRBs occurs on timescales of mere milliseconds - and sometimes only span microsecond timescales. The mechanism that can produce such powerful bursts on surprisingly short timescales is not yet known - magnetars and interactions involving magnetars are among the popular theory, but work is ongoing in developing and testing FRB progenitor models. Complicating the matter is the possibility that there are multiple progenitor mechanisms for FRBs (see review by Cordes and Chatterjee, 2019).

FRBs are a relatively new field of astronomy. The first FRB was discovered in 2007 (Figure 1), from archival data previously obtained by the Murriyang/Parkes radio telescope (Lorimer et al., 2007). The signal was 10–12 orders of magnitude brighter than any other radio signal known at the time, and had a high implied distance, placing the progenitor as an extragalactic source (Lorimer et al., 2024). It took

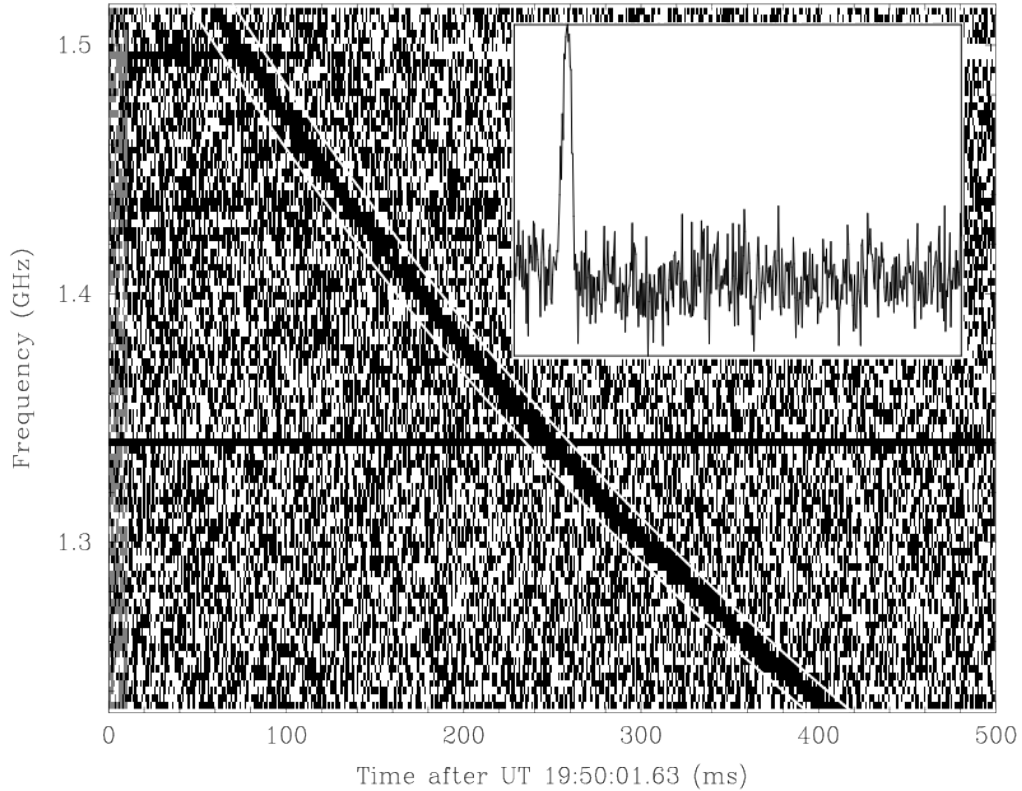


Fig. 1: The Lorimer Burst, the first FRB detected. The FRB is dispersed across the frequency band and broadens at lower frequencies. Inset: the total-power signal of the de-dispersed pulse assuming a dispersion measure of 375 pc cm^{-3} . Image source: Lorimer et al. (2007).

until Thornton et al. (2013) for further FRBs to be identified with Parkes, confirming the existence of a population of FRBs. Spitler et al. (2014) then followed with the first FRB detection within Arecibo radio telescope archival data - the first FRB not detected by Parkes. Lorimer et al. (2024) points out that improvements in detecting such pulses, first demonstrated in McLaughlin and Cordes (2003) through a single-pulse search code, rather than a Fourier transform approach for periodic pulses, was key to the initial discovery of FRBs. Additionally, improvements in computational resources at the time had developed sufficiently to enable the search for bright single pulses in large datasets ‘over a period of a few months’ (pg 7 of Lorimer et al., 2024).

1.1 FRB surveys

Since the confirmation of FRBs as extragalactic phenomena, this field of research has exploded, with numerous surveys underway and telescopes used in the search and follow-up of FRBs. While other archival datasets of Parkes have been searched for further FRB signals with some detections made, it has arguably seen more success in follow-up of known repeating FRB signals, especially since the addition in an ‘Ultra wideband receiver’, allowing for continuous coverage of 0.7–4.0 GHz (Hobbs et al., 2020). The Five-hundred-meter Aperture Spherical Telescope (FAST) telescope has greater sensitivity than the 64 m dish at Parkes and has also granted new insights into repeating signals, and discovered new FRBs. However, the majority of FRB detections to-date have been made by the Canadian Hydrogen Intensity Mapping Experiment (CHIME) radio telescope. 536 have been published in the CHIME/FRB Catalog 1 alone (CHIME/FRB Collaboration et al., 2021), with thousands more expected to be published in due course.

A key point to highlight is that these telescopes — with localization uncertainties of several arcminutes — currently lack the ability to localize FRBs to their host galaxies unless they have been seen to repeat several times. As most FRBs to date have been seen only as one-off bursts, localizations of several arcminutes are insufficient to identify a host galaxy and hence obtain a distance measurement to the FRB - a crucial component for the use of FRBs as probes of cosmology, as explained below. CHIME does plan to address this through the addition of ‘outrigger’ telescopes (Lanman et al., 2024), which will enable a significant fraction of CHIME-detected FRBs to be precisely localized on the sky. Meanwhile, more conventional interferometric radio telescopes have taken the lead in this area. The Commensal Real-time ASKAP Fast Transient (CRAFT) survey has recently reported 30 FRBs localized to an identifiable host galaxies, at sub-arcsecond precision (Shannon et al., 2024), with the Australia Square Kilometre Array (SKA) Pathfinder telescope. Figure 2 shows one of the CRAFT localizations, for FRB 20211127I. The CRAFT FRB detection and localization rate is projected to significantly increase by an order of magnitude through the use of a coherent-mode real-time search system. The Deep Synoptic Array (DSA-110) meanwhile reported 11 localizations (Law et al., 2024) for a sample of 25 FRBs (Sherman et al., 2024), with a factor of ~ 2 lower precision but sufficient to identify the host galaxies of several FRBs. Sharma et al. (2024) thereafter presented localizations and redshifts for 30 FRBs total, for

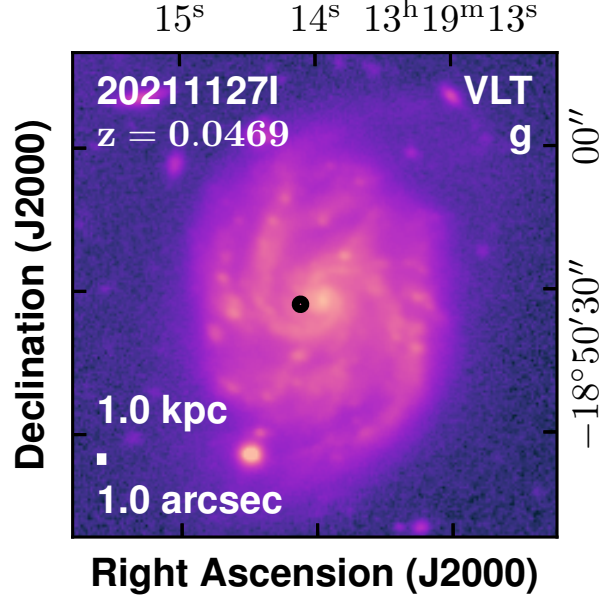


Fig. 2: An example of the localization region (black ellipse) for FRB 202111271 by ASKAP overlaid on VLT imaging obtained following the FRB localization (Glowacki et al., 2023). For sufficiently nearby FRBs with sub-arcsecond precision on the FRB position, not only can the host galaxy be identified, but what part of the galaxy the FRB occurred in - essential for studies of the local environment of the progenitor. Image source: Shannon et al. (2024); image credit: Lachlan Marnoch.

FRBs detected up to November 2023. DSA-2000, an upgrade of DSA-110, will also greatly increase its detection and localization rate when constructed. The MeerTRAP (More Transients and Pulsars) survey with the Meer Karoo Array Telescope (MeerKAT) instrument is another FRB detection and localization survey which is also able to achieve sub-arcsecond precision, as demonstrated by Driessen et al. (2024). Complemented by localizations of repeating FRBs, there are over 70 well-localized FRBs to date, spanning from galaxies within the Local Group to beyond redshifts of $z = 1$ (Ryder et al., 2023; Connor et al., 2024).

For cosmological studies, redshift measurements of the host galaxies of FRBs are a crucial detail to couple with the dispersion measure (DM), which can be readily measured for both pulsars and FRBs.

2 Dispersion Measure

As electromagnetic waves propagate through a ionized plasma, they experience interactions that induces a delay on the group frequency that depend on the photon energy. For a broadband signal originating from a cosmological redshift z , this induces differences in the observed arrival time, Δt , between photons with different frequencies ν_1 and ν_2 , where

$$\Delta t = \frac{e^2}{2\pi m_e c} \left(\frac{1}{\nu_1^2} - \frac{1}{\nu_2^2} \right) \int \frac{n_e(l)}{1+z_l} dl \approx 0.415 \text{ s} \left[\left(\frac{\nu_1}{\text{GHz}} \right)^{-2} - \left(\frac{\nu_2}{\text{GHz}} \right)^{-2} \right] \frac{\text{DM}}{10^2 \text{ pc cm}^{-3}}, \quad (1)$$

where e is the electron charge, m_e and n_e are the mass and number density of electrons, respectively, c is the speed of light, and l is the proper path element. The dispersion measure, DM, is the more commonly-used physical quantity,

$$\text{DM} \equiv \int \frac{n_e(l)}{1+z_l} dl, \quad (2)$$

i.e. the proper integral over the free electrons density intersected at redshift z . For sources in the $z < 0.1$ Local Universe with $\text{DM} \sim 100 \text{ pc cm}^{-3}$, the time delay is less than a second, which means that the observed signal has to be in discrete pulses with much shorter durations in order for the time delay to be measurable.

These relations were first derived by Ginzburg (1973) not long after the first discovery of pulsars by Jocelyn Bell Burnell in 1968. While Ginzburg proposed that (then-)hypothetical extragalactic radio sources could be used to probe the cosmic gas distribution, in the following decades DMs were measured primarily from pulsars within the Milky Way, which proved to be a crucial probe of the ionized gas structure in the Milky Way disk (Cordes, 2004). While a small number (~ 30) of pulsars have been detected in the Small- and Large-Magellanic

Clouds (SMC and LMC, satellite galaxies of the Milky Way at distances of $D \sim 50 - 60$ kpc), at the time of writing no pulsars have been detected at greater distances.

2.1 The Cosmic Dispersion Measure

Around the turn of the millennium, GRBs — short, intense, bursts of gamma ray emission powered by distant supermassive black holes — was a phenomenon of intense interest in astrophysics, and there were hopes that associated radio transients might be detected from GRBs. At around the same timeframe, the overall Λ CDM cosmological paradigm became firmly established thanks to the discovery of the accelerating Universe using Type Ia supernovae as well as precision CMB measurements from WMAP. With the overall cosmic energy budget measured to within $\sim 10\%$ by the early 2000s, these developments motivated Ioka (2003) and Inoue (2004) to separately derive estimates of the mean cosmic DM contribution, $\langle \text{DM}_{\text{cosmic}} \rangle(z)$ as a function of source redshift, that would be expected from a generic radio source with measurable DM. This can be derived by inserting \bar{n}_e^{diff} , the mean value for the diffuse free electron density of the Universe, into Equation 2. This is calculated by counting the electrons contributed by cosmic hydrogen and helium at the critical (i.e. mean cosmic) matter density of the Universe:

$$\bar{n}_e^{\text{diff}} = f_{\text{diff}} \Omega_b \left[\frac{m_{\text{He}}(1 - Y) + 2Ym_{\text{H}}}{m_{\text{H}}m_{\text{He}}} \right] \bar{\rho}_c, \quad (3)$$

where f_{diff} is the overall fraction of diffuse cosmic baryons traversed by the sightline across the IGM and CGM (f_{diff} is in principle also a function of redshift). The factor in square parentheses corrects for the contributions of helium, which comprise $Y = 0.243$ the total baryonic mass of the Universe and contribute 2 electrons per nucleon instead the solitary electron from hydrogen — m_{H} and m_{He} are the atomic masses of hydrogen and helium, respectively. This expression implicitly assumes that the diffuse cosmic gas is fully ionized, which is a reasonable assumption since the cosmic fraction of neutral hydrogen in the IGM/CGM has been measured at only $\Omega_{\text{HI}} \sim 10^{-4}$ (see, e.g., Neeleman et al. 2016), i.e. the neutral fraction of cosmic baryons is only $\Omega_{\text{HI}}/\Omega_b \sim 1\%$ outside of visible galaxies (with the order-of-magnitude assumption that hydrogen constitutes most of the cosmic baryons, $\Omega_b \sim \Omega_H$). One can also safely neglect the contribution of ‘metals’ with atomic numbers above 2: the cosmic abundance of lithium, the next-most abundant primordial element, is merely $\approx 5 \times 10^{-10}$ that of hydrogen. Meanwhile, the most abundant element produced in stellar processes, oxygen, has an abundance of $\sim 10^{-4}$ relative to hydrogen in the most metal-enriched galaxies in the Universe. Even if one were to (wrongly) assign such extreme metallicities to the entire cosmic baryon distribution, it would modify the electron density in Equation 3 by only $\sim 0.1\%$. At redshifts prior to the full reionization of hydrogen ($z \gtrsim 7$) or Helium-II ($z \gtrsim 3$), further scale factors are required to correct for the respective neutral fractions; these neutral fractions can in principle be constrained with future samples of FRBs if they can be detected at sufficiently high redshifts. Finally, $\bar{\rho}_c(z_l)$ is the critical density of the universe at the redshift z_l . If f_{diff} is approximated to have no redshift dependence, $\bar{\rho}_c$ is the only quantity with redshift or distance dependence in Equation 2, allowing the integral to be evaluated as a function of redshift by substituting the Hubble relation. While the exact values for $\langle \text{DM}_{\text{cosmic}} \rangle(z)$ depend on the cosmological parameters as well as assumptions on f_{diff} , most models predict $\langle \text{DM}_{\text{cosmic}} \rangle(z) \sim 1000 z$ (a useful rule-of-thumb!) at $z < 1$, for plausible values of $f_{\text{diff}} \sim 0.7 - 0.9$.

While radio signals associated with GRBs have yet to be detected at the time of writing (although afterglows are seen in the radio), it was the discovery of FRBs that opened up the use of the cosmic DM as a probe of the cosmological baryon distribution.

3 The missing baryon problem and the Macquart relation

3.1 Missing in action

The presence of helium and deuterium in the Universe is a key piece of evidence in favor of the Big Bang, since they cannot be produced in sufficient quantities by any known stellar processes to account for the observed abundances. Instead, they had to be created from neutron and proton fusion at very high temperatures ($T \sim 10^9$ K) several minutes after the Big Bang. The analysis of relative yields of the resulting light elements, known as the technique of Big-Bang Nucleosynthesis (BBN), is highly sensitive to the overall baryon (i.e. proton and neutron) density of the Universe, and yield precise predictions that $\Omega_b h^2 \approx 0.022$. In other words, only 4% of the mass-energy budget of the Universe are in baryons assuming $h \approx 0.7$, where $h \equiv H_0/(100 \text{ km s}^{-1})$ is the Hubble parameter.

Assuming Ω_b is known through BBN, one can write down the different fractional contributions to the total cosmic baryon budget:

$$f_{\text{diff}} + f_* + f_{\text{ISM}} + f_{\text{bh}} = 1, \quad (4)$$

where f_* is the fraction residing in visible stars within galaxies; f_{ISM} is the fraction as ISM gas, also within galaxies, usually estimated through emission lines in star-forming nebulae as well as molecular gas from the sub-mm radio observations; f_{bh} is the fraction believed to have collapsed into black holes. f_{diff} is the diffuse component which can further be separated into:

$$f_{\text{diff}} \equiv f_{\text{IGM}} + f_{\text{CGM}} + f_{\text{IGrM}} + f_{\text{ICM}}, \quad (5)$$

where f_{IGM} is the large-scale IGM contribution from the large-scale cosmic web at low matter overdensities; f_{CGM} , from the circumgalactic medium gas around low- to intermediate-mass galaxies with $M_{\text{h}}/M_{\odot} \lesssim 10^{13}$; f_{IGrM} from $M_{\text{h}}/M_{\odot} \sim 10^{13} - 10^{14}$ galaxy groups; and f_{ICM} represents the contribution from the aggregate intra-cluster media of massive galaxy clusters with $M_{\text{h}}/M_{\odot} \gtrsim 10^{14}$. This decomposition of f_{diff} reflects a specific ansatz on the astrophysics that affect the cosmic gas across different overdensity regimes (see Sections 4.1 and 4.2); it might be more useful to vary the exact categorizations for different model assumptions.

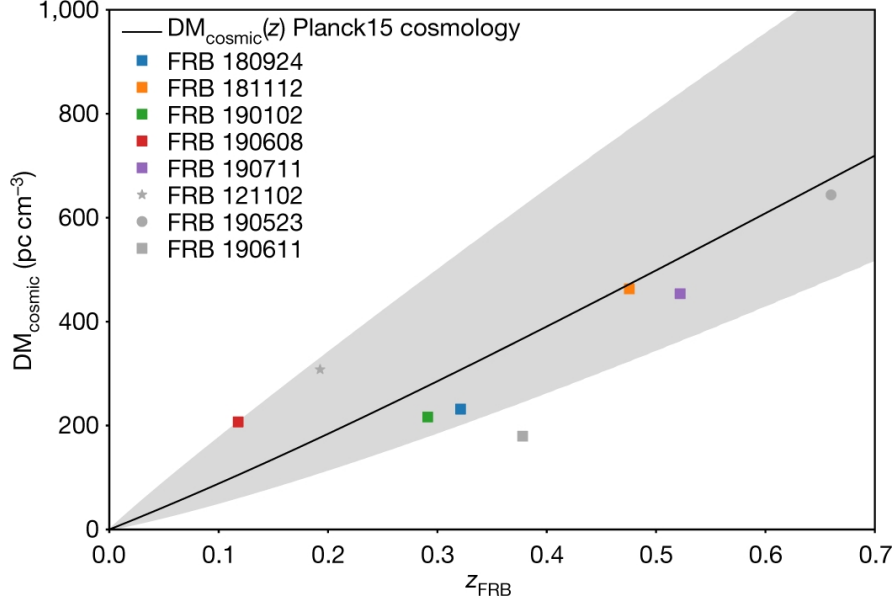


Fig. 3: The first measurement of the ‘missing baryons’, where the cosmic DM is plotted against the spectroscopic redshift of well-localized FRBs (Macquart et al., 2020). The solid line is the expected relation based on the Planck Collaboration et al. (2020) relation. The shaded region encompasses 90% of the DM_{cosmic} values from a model for ejective feedback in Galactic halos motivated by simulation.

By the turn of the millennium, observational astronomy had advanced to the point where Fukugita et al. (1998) were able to make a census, by compiling different observations, of the relative baryon fractions (Equation 4) of the Local Universe. The later meta-analysis by Fukugita and Peebles (2004) revealed that only $f_* \sim 6 - 7\%$ of the cosmic baryon budget could be accounted for by stars observed in galaxies, while another $f_{\text{ICM}} \sim 4 - 5\%$ were within the hot $T \sim 10^7$ K X-ray emitting intracluster medium (ICM) gas permeating massive galaxy clusters ($M \gtrsim 10^{14} M_\odot$). The rest of the 90% of the cosmic baryons had to reside outside of galaxies and clusters, either in the circumgalactic media (CGM) surrounding galaxy halos on ~ 100 kpc scales or in the average- to low-density intergalactic medium (IGM) tracing the cosmic web on the largest scales of the Universe. However, these baryons were ‘missing’ in the sense that they were not observationally detected in the Local Universe using straightforward methods. Ironically, during ‘Cosmic Noon’ ($z \sim 2 - 5$) where the hydrogen 121.6 nm Lyman- α line is redshifted into optical wavelengths accessible from ground-based telescopes, all of the intergalactic baryons are accounted-for in the Lyman- α forest, which is primarily caused by trace amounts of neutral hydrogen maintained at optically-thin photoionization equilibrium at a relatively cool $T \sim 10^4$ K. As large-scale structure evolves with time, primarily through gravitational collapse, the entrained gas heats up from collisional shock-heating and feedback from galaxies, eventually rendering them invisible in the Lyman- α forest.

Cosmological hydrodynamical simulations (e.g., Davé et al. 2001; Cen and Ostriker 2006) suggested that a large portion of this gas is likely to reside in a state dubbed the warm-hot intergalactic medium (WHIM) at temperatures of $T \sim 10^{5-6}$ K (Cen and Ostriker, 1999). This straddles the regime where the gas might be cool enough to show up in absorption either in hydrogen or metals (e.g., Mg II) against background quasars, or sufficiently hot and dense to emit significantly in X-rays. Nevertheless, through different absorption lines in both the ultraviolet (e.g., Werk et al., 2014) and X-ray (e.g., Nicastro et al., 2018) occupying various phases of the CGM and IGM, heroic efforts were made to account for the missing baryons. The patchwork nature of these studies are exacerbated by the fact that the conversion of these absorption line statistics into baryon fractions require considerable modeling assumptions about the metallicity, temperature, ionizing background, equilibrium conditions, turbulence, and other properties of the gas. As of 2019, meta-analyses suggested that approximately $\sim 20\%$ of the cosmic baryons were still unaccounted for (de Graaff et al., 2019), but the uncertainties were sufficiently large to allow for up to $\sim 50\%$ of undetected cosmic baryons, or for all of them to already be accounted for.

3.2 The Macquart Relation

As described in Section 1.1, FRB detection and localization has only recently grown to significant levels for this relatively new field of research. The CRAFT survey, with the ASKAP radio telescope, was the first project to demonstrate the ability to localize multiple one-off FRBs to their host galaxies. In Macquart et al. (2020), four new localizations were reported, bringing the total published number of localized FRBs to nine at that point. This sample was large enough to conduct the first direct measurement of the baryon content of the Universe, performed using the dispersion measure of this sample of localized FRBs, combined with the spectroscopic redshift measurements of their host galaxies.

In Figure 3, a clear relationship is shown between the cosmic DM (DM_{cosmic} , the amount of dispersion attributed to the space between the Milky Way and the FRB host galaxy and corresponding halos) versus the redshift z of the identified host galaxies, even for a modest

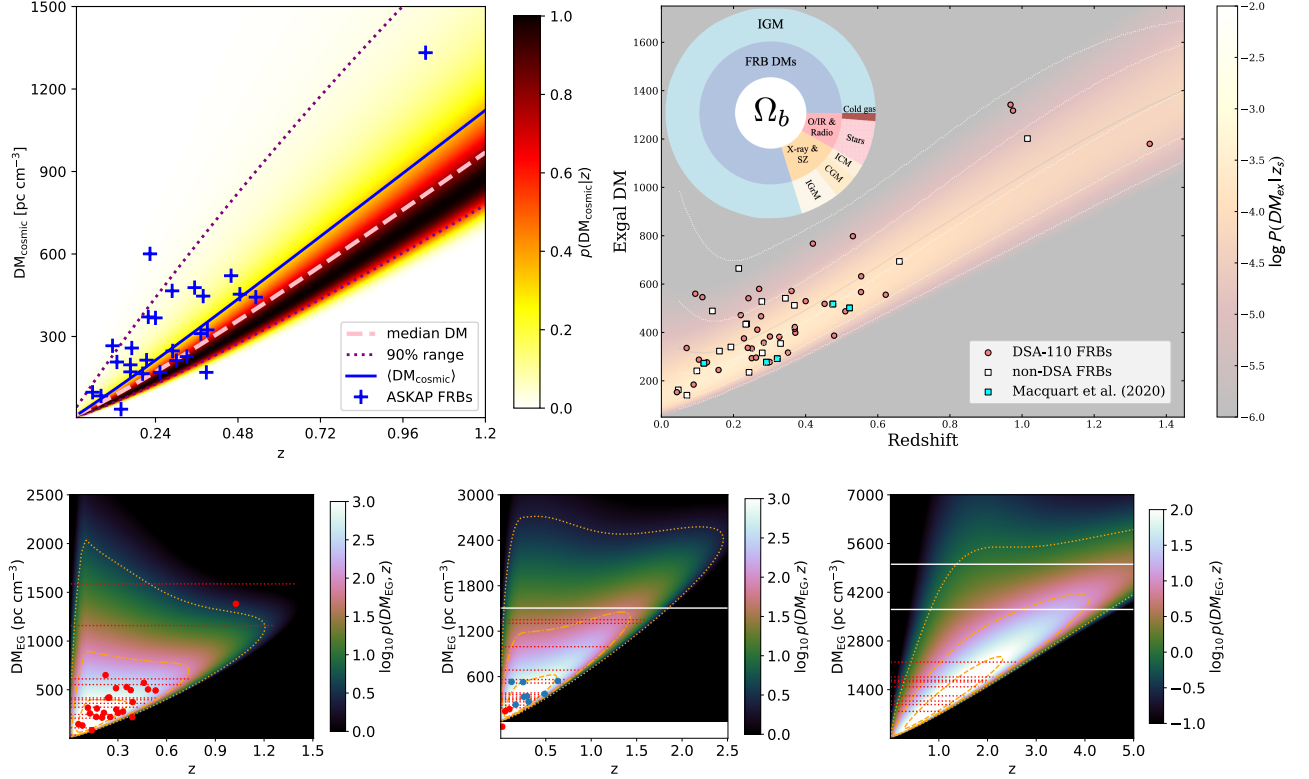


Fig. 4: Macquart relation distributions from various FRB surveys. Top left: The Macquart relation (solid line) for the CRAFT incoherent-spectrum survey, with shading indicating the probability density of the DM for the cosmic web DM_{cosmic} (Shannon et al., 2024). Top right: The Macquart relation for the DSA-110 FRBs considered alongside other FRBs in the literature, presented in Connor et al. (2024). The radial treemap insert shows a partition of cosmic baryons produced by combining the FRB distribution with other precision probes of baryons in the Universe. Bottom row: Predictions for the Macquart relation for CRAFT (left), DSA-110 (middle), and FAST (right). These are derived using best-fit parameters described in Hoffmann et al. (2024). DSA-110 is predicted to detect 2–12% at $z > 1$, and FAST expected to detect 25–41% of their FRBs at $z > 2$. Image credits: Clancy James, Liam Connor, Jordan Hoffmann.

number of five localized FRBs (where three other FRBs were also included on the figure, two also included in further calculations presented in Macquart et al., 2020). What has now been termed as the Macquart relation describes the correlation between these two measurements. The solid line in the plot gives the expected relation based on the Planck Collaboration et al. (2020) cosmology, while the shaded region encompasses 90% of the DM_{cosmic} values from a model for ejective feedback in Galactic halos motivated by simulations (see Section 3.3). The observed scatter is largely consistent with the scatter from the intergalactic medium: ‘effectively, the FRB measurements confirm the presence of baryons with the density estimated from the CMB and BBN, and these five measurements are consistent with all the missing baryons being present in the ionized intergalactic medium’ (pg 6 of Macquart et al., 2020). This was the solution to the ‘missing baryon problem’, the first detection of hot ionized gas which had evaded approaches such as X-ray observations.

The result of Macquart et al. (2020) is, however, far from the last on the matter on missing baryons. The DM from FRBs only gives the total amount of ionized electrons along the line of sight. The DM measurement alone does not inform us where the hot ionized gas is exactly distributed, after accounting for the contributions from the FRB host galaxy or the Milky Way. Even these two are not well constrained and are often assumed. The amount of DM from these contributors is not unconstrained enough to place doubt on the Macquart relation, but with plenty of room for improvement necessary to place firm constraints on cosmological parameters. An example is seen by Ravi et al. (2023), where the DSA-110 telescope localized an FRB to a nearby spiral galaxy at a mere 50 Mpc away. Conservative upper limits on the Galactic CGM contribution to the total DM of $28.7\text{--}47.3\text{ pc cm}^{-3}$, which hence enables an upper limit to be placed on the mass of baryons in the Galactic CGM. Yet, as highlighted in table 4 of Hoffmann et al. (2024), the total observed DM reported by Ravi et al. (2023) of 110.96 pc cm^{-3} is less than the DM contribution estimated from the Milky Way ISM alone through the NE2001 model (Cordes, 2004), of 126.77 pc cm^{-3} . A negative DM_{cosmic} contribution is obviously nonphysical (see also Figure 4 bottom-middle panel), demonstrating that improvements on our ability to measure specific contributions to the total DM is a necessity.

Another area of improvement is in extending the sample of localized FRBs to significantly larger sizes. Shannon et al. (2024) repeats the measure for the CRAFT ICS survey FRBs (a sample of 30 well-localized FRBs), noting areas where improvements could be made - for example, two FRBs are seen to lie well below the minimum expectation in their observed DM, which is attributed to small host contributions,

under-fluctuations in Milky Way contributions, or a combination of both. Connor et al. (2024) also highlights an updated Macquart relation, using both their sample of DSA-110 localized FRBs and some of the localizations presented in the literature. With this large cosmological sample of FRBs localized to host galaxies, they leveraged the IllustrisTNG hydrodynamical simulation to partition previously missing baryons into the IGM, galaxy clusters, and galaxies, and hence estimate a total baryon density of the Universe. Predictions of the Macquart relation for both these surveys and for FRBs detected with FAST, as well as fitting of cosmological parameters, were presented by Hoffmann et al. (2024) (Figure 4), based on the population of existing detections and modeling of the instrumental biases for each survey. This work predicted that DSA-110 will find as many as 12% of its FRBs at $z > 1$, and for FAST 25–41% of its detected FRBs will arise from $z > 2$ host galaxies.

3.3 The Distribution of DM_{cosmic}

The observed FRB signals do not traverse a uniform cosmic medium, but rather pass through fluctuations in the gas structures along the line-of-sight. An ensemble of FRBs at exactly the same redshift would exhibit a finite distribution of DM_{cosmic} values depending on the over- and under-densities of the IGM that have been traversed, as well as chance intersections with CGM halos in foreground galaxies. At first glance, the variance caused by this distribution, $p(DM_{\text{cosmic}})$, might be regarded simply as a source of uncertainty for measuring the Macquart relation ($\langle DM_{\text{cosmic}} \rangle$ versus z), but it is a potentially rich source of information in its own right since it encodes the variance of gas in the Universe. In the simplest approximations where the ionized baryon distribution simply traces the underlying matter density field through a linear scale factor like f_{diff} in Equation 3, the only other parameters governing $p(DM_{\text{cosmic}})$ are the underlying cosmological parameters, including Ω_b as well as Ω_m , the matter density fraction, and σ_8 , the amplitude of matter fluctuations. However, with galaxy feedback from supernovae and AGN likely to eject gas from galaxies into the halo CGM and possibly as far as the IGM on Mpc scales, the cosmic baryon distribution is likely to be modulated relative to that of the overall matter density field (see Section 4).

Macquart et al. (2020) introduced a commonly-used functional form for $p(DM_{\text{cosmic}})$:

$$p(\Delta_{\text{cosmic}}) = A \Delta_{\text{cosmic}}^{-\beta} \exp \left[-\frac{(\Delta_{\text{cosmic}}^{-\alpha} - C_0)^2}{2\alpha^2 \sigma_{\text{DM}}^2} \right], \quad (6)$$

where $\Delta_{\text{cosmic}} \equiv DM_{\text{cosmic}} / \langle DM_{\text{cosmic}} \rangle$, while A , α , β , σ_{DM} , and C_0 are free parameters in the model. This functional form was chosen to ensure that $p(DM_{\text{cosmic}})$ behaves intuitively at certain limits. α and β encode the gas profiles of the population of foreground galaxy halos. $\alpha \approx 3$ and $\beta \approx 3$, found to be consistent with simulations in Macquart et al. (2020), are commonly-used values in the literature although they are likely to be dependent on galaxy feedback models (see Section 4 below). The variance of this distribution is largely regulated by σ_{DM} . In the limit of small σ_{DM} , the cosmic structures are generally in the linear regime of gravitational collapse (scales of $\gtrsim 10$ Mpc) and should therefore trend toward a Gaussian distribution. This formulation is also designed to reproduce the two limiting regimes of the expected $p(DM_{\text{cosmic}})$ distribution: at low- DM_{cosmic} , there is a sharp cut-off due to the diffuse IGM, while at large- DM_{cosmic} there is a long tail due to the rare sightlines that intersect massive foreground halos with large DM contributions. Finally, A and C_0 are normalization constants such that the mean of $p(DM_{\text{cosmic}})$ reproduces the mean Macquart relation as a function of redshift, i.e. they are dependent on Ω_b as well as the total amount of diffuse baryons, f_{diff} .

Other than $\langle DM_{\text{cosmic}} \rangle(z)$, the parameter that can modify the $p(DM_{\text{cosmic}})$ of Equation 6 the most at a given redshift is σ_{DM} . Recent analyses often parametrize this through $F(z) = \sigma_{\text{DM}} \sqrt{z}$, which assumes that the variance in $p(DM_{\text{cosmic}})$ scales with redshift due to a Poisson-like probability of intersecting foreground halos. However, future analyses of $p(DM_{\text{cosmic}})$ would likely require the realism provided cosmological hydrodynamical simulations, perhaps using machine-learning techniques to directly emulate the functional form of $p(DM_{\text{cosmic}})$ predicted by the simulations.

3.4 Deconstructing the FRB DM

As an alternative to analyzing the overall distribution of DM_{frb} at a given redshift, one can also write down the expected contributions to the overall FRB dispersion:

$$DM_{\text{frb}} = DM_{\text{MW}} + DM_{\text{IGM}} + DM_{\text{halos}} + DM_{\text{host}} / (1 + z_{\text{frb}}), \quad (7)$$

where the emitted radio waves are firstly dispersed by the (unknown) FRB engine and host galaxy (DM_{host} , usually defined in the FRB rest-frame), before traversing the diffuse gas of the filamentary cosmic web (at low-to-moderate matter overdensities of $0 \lesssim \rho_m / \bar{\rho}_m \lesssim 10$) which imprints the IGM contribution, DM_{IGM} . The sightline might also intersect the CGM gas from foreground halos, $DM_{\text{halos}} = \sum_i DM_{\text{halo},i} / (1 + z_i)$, that might be further decomposed into the individual halo contributions $DM_{\text{halo},i}$ (note no plural in the subscript for individual halos) in their respective restframes. As defined in Section 2.1, $DM_{\text{cosmic}} \equiv DM_{\text{IGM}} + DM_{\text{halos}}$, but note that some papers use the notation ‘ DM_{IGM} ’ with the same meaning as our DM_{cosmic} , i.e. they do not distinguish between the IGM and halo gas. Finally, the signal enters the Milky Way and is dispersed by the gas in its halo and disk, leading to DM_{MW} .

Based on DM measurements with Galactic pulsars and models of the Milky Way ISM structure, there exist reasonable models of the Milky Way disk contribution as a function of position on the sky (Cordes, 2004; Yao et al., 2017), with a mean contribution of $DM_{\text{MW,disk}} \sim 30 \text{ pc cm}^{-3}$ at latitudes $b > 10^\circ$ away from the Galactic plane. There should also be a contribution from the extended CGM of the Milky Way halo, which was estimated by (Prochaska and Zheng, 2019) to be $DM_{\text{MW,halo}} \approx 50 \text{ pc cm}^{-3}$, although this is still uncertain; different models of the Milky Way CGM would predict different values. Nearly all DM analyses of extragalactic DM therefore directly subtract the Milky Way contribution as a first step, with the associated uncertainties added into the error analysis. This leads many papers to define the ‘extragalactic’ DM, $DM_{\text{eg}} = DM_{\text{frb}} - DM_{\text{MW}}$, as the contribution from everything beyond the Milky Way halo.

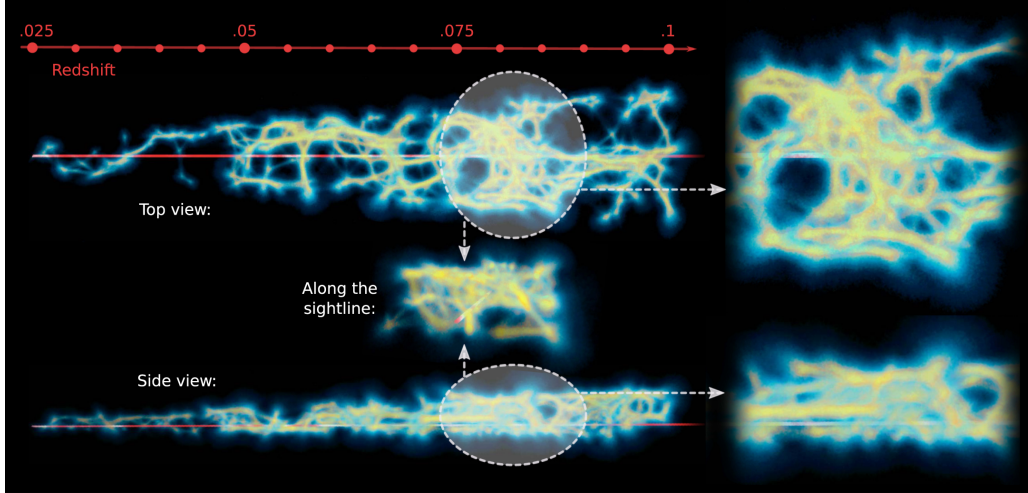


Fig. 5: A visualization of the cosmic web reconstructed from SDSS spectroscopic survey data in the foreground of FRB201900608A, which was localized to a FRB at $z = 0.117$. This allowed a specific value of DM_{IGM} to be calculated, which enabled the first assessment of an extragalactic FRB’s DM budget (Simha et al., 2020). Credit: Sunil Simha.

The host component, DM_{host} , is usually defined as the combined contributions from the host galaxy ISM and CGM as well as the (unknown) FRB engine. A common assumption is that the DM_{host} of most FRBs is dominated by the host galaxy ISM and halo, such that its rest-frame value is comparable to that of the Milky Way, i.e. $DM_{\text{host}} \sim 50 - 100 \text{ pc cm}^{-3}$. This rough value is supported by analyses that constrain $\langle DM_{\text{host}} \rangle$ as a free parameter (James et al., 2022). However, a subset of localized FRBs exhibit DM_{eg} that are well in excess of $\langle DM_{\text{cosmic}}(z_{\text{frb}}) \rangle$ given their redshifts. One of the most well-known cases, FRB20190520B at $z_{\text{frb}} = 0.24$, was measured with $DM_{\text{frb}} = 1205 \text{ pc cm}^{-3}$ (Niu et al., 2022; Ocker et al., 2022) which implies a huge $DM_{\text{host}} \approx 900 \text{ pc cm}^{-3}$ after subtracting off DM_{MW} and $\langle DM_{\text{cosmic}}(z = 0.24) \rangle$. The subsequent discovery that this FRB sightline intersects the ICM of two separate galaxy clusters has led to a downward revision of the estimated host contribution to $DM_{\text{host}} \sim 300 - 400 \text{ pc cm}^{-3}$ (Lee et al., 2023), which is still well in excess of the $\langle DM_{\text{host}} \rangle \sim 100 \text{ pc cm}^{-3}$ seen in the bulk of the FRB population. In their cross-correlation analysis of 492 unlocalized CHIME FRBs with galaxy imaging surveys, Rafiei-Ravandi et al. (2021) found that their results implied that a sub-population of FRBs must have excess DM_{host} values. They speculated that these high-DM FRBs are hosted within galaxy cluster halos ($M_h \gtrsim 10^{14} M_{\odot}$). Subsequently, Connor et al. (2023) reported two localized high-DM FRBs that were indeed embedded within galaxy cluster halos, although Simha et al. (2023) studied several other localized FRBs with large DM_{host} values that are not associated with massive halos. Therefore, at least some of the excess- DM_{host} FRBs are caused by dense gas much closer to the FRB than their extended host galaxy halos, and it is still unknown whether these objects have similar mechanisms as other FRBs.

The $DM_{\text{cosmic}} \equiv DM_{\text{IGM}} + DM_{\text{halos}}$ components are often modeled statistically based on the distribution of large-scale structure and galaxy halos either from (semi)-analytic theory or simulations (see Section 3.3). This is especially the case for unlocalized FRBs where the positional uncertainty precludes a precise census of the diffuse intergalactic foreground contributions. However, given detailed spectroscopic observations, it is possible to separately model DM_{IGM} and DM_{halos} . This was first attempted by Simha et al. (2020) who analyzed FRB20190908A, a FRB localized to a $z_{\text{frb}} = 0.117$ host galaxy. Using the DM_{halos} estimated from deep spectroscopy with the Keck-I telescope as well as DM_{IGM} calculated from the reconstructed cosmic web based on SDSS spectroscopic data, they were able to show that the calculated sum of their model DM budget (right side of Equation 7) was consistent with the observed DM_{frb} to within the uncertainties, which were admittedly sizeable.

In particular, Simha et al. (2020) had made specific assumptions on the CGM gas fractions and IGM baryon fraction, f_{IGM} , which are in reality unknown quantities that can be constrained by larger samples of qualitatively similar data sets. Motivated by this, the FRB Lightcone Ionization Measurement From Lightcone AAOmega Mapping (FLIMFLAM) project (Huang et al., 2024) aims to obtain comprehensive spectroscopic data in the foregrounds of $\sim 20 - 30$ localized FRB fields at $z_{\text{frb}} < 0.5$, through dedicated observations with various ground-based multi-object spectroscopic facilities as well as leveraging public spectroscopic surveys such as SDSS and 6dF (Lee et al., 2022). The direct modeling of the various components in Equation 7 for individual FRB sightlines is forecasted to enable $\sim 10\%$ constraints on the parameters governing the IGM and CGM baryon fractions (see Sections 4.1 and 4.2) in samples of ~ 30 FRBs. The analysis of the initial FLIMFLAM data release of 8 FRB fields (Khrykin et al., 2024a) has yielded the first direct constraints on the IGM baryon fraction, $f_{\text{IGM}} = 0.59^{+0.11}_{-0.10}$, as well as separating out contributions from the ‘unknown’ host galaxy ISM and FRB engine, $DM_{\text{host}}^{\text{unk}} = 69^{+28}_{-19} \text{ pc cm}^{-3}$ from the host halo component. Data from the new generation of multiplexed spectroscopic facilities, such as DESI and Subaru PFS, will harvest foreground data on hundreds of localized FRBs within the next several years, allowing percent-level constraints on the cosmic baryon distribution.

Finally, we note that every term in Equation 7 has a non-Gaussian distribution, with significant skew and kurtosis. Given that most statistical methods are developed with the Gaussian distribution in mind, the non-Gaussianity of $p(DM_{\text{cosmic}})$ and its constituent parts

makes inference in FRB cosmology highly challenging. A non-negligible fraction of the FRB cosmology literature assumes Gaussian statistics anyway, thus their conclusions should be taken with a pinch of salt. In general, the more external information can be garnered on the different DM components, the better.

4 Probing the Cosmic Baryon Distribution

The Macquart et al. (2020) result showed that the cosmic DM probed by FRBs is consistent with the Ω_b from cosmological analyses, but conceptually many of the questions related to the missing baryon problem remain: where do the baryons reside in the Universe, and what can we learn from this? In the absence of any baryonic pressure or galaxy feedback, approximately 50% of all cold dark matter collapses into galactic haloes, occupying scales of $\sim 100 - 200$ kpc for Milky Way-like galaxy halos. However, baryons are not collisionless, meaning that gas collapsing through gravitational forces can get heated up and shocked as they move. Furthermore, some baryons in galaxies might additionally get ejected into the CGM and IGM due to galaxy feedback. FRBs have much potential to reveal this complex interplay between gas accretion and feedback through the cosmic gas distribution, yielding insights into the processes that regulating galaxy evolution. At the same time, the redistribution of gas between the CGM of various halo masses and the IGM can alter the large-scale matter distribution with consequences for the interpretation of cosmological measurements.

4.1 Cosmological Hydrodynamical Simulations and FRB Analysis

The FRB DM is a unique probe of the IGM baryons tracing the low-density cosmic web at low redshifts, that constitute the majority of the cosmic baryon budget but elude direct detection by other observational techniques. In order to gain theoretical insight into this, however, numerical simulations are required especially to study incorporate the effect of gas feedback from galactic processes.

While dark matter-only N -body simulations have been a critical tool for understanding the growth of large-scale structure, they do not incorporate the gas physics required to directly model the cosmic baryons. Hydrodynamical simulations that do track the gas are much more computational intensive, and typically cover much smaller box sizes than feasible with dark matter-only simulations. Early generations of cosmological hydrodynamical simulations, which helped elucidate the nature of the Lyman- α forest and WHIM (see Section 3), typically did not have the resolution or subgrid modelling to track the growth and evolution of individual galaxies, and used highly simplified prescriptions for feedback (if any). Since the turn of the millennium, however, cosmological hydrodynamical simulations have aimed to simultaneously cover sufficiently large volumes ($L \gtrsim 10$ Mpc) to trace the evolution of large-scale structure both in dark matter and gas, while also capturing the evolution of a statistical sample of individual galaxies (and indeed galaxy clusters) within said volume. In order to be computationally tractable, these require subgrid physics models to capture processes occurring on scales below the simulation resolution (typically $\sim 0.1 - 1$ kpc at the time of writing). The resulting galaxy populations have realistic-looking morphologies and other properties including metallicities, gas thermal properties, and even magnetic fields. Even in the earlier simulations, however, one useful ansatz had emerged which is now applicable to FRB studies: the gas in the IGM is generally a linear tracer of the low-density cosmic web. Thus one can generalize Equation 3 to apply to local fluctuations of the free electron density instead of just the cosmic mean density, i.e. $n_e(x) = f_{\text{IGM}}(\Omega_b/\Omega_m) A_Y \rho_m(x)$, where A_Y is the factor in square parentheses in Equation 3 which accounts for the helium contribution, and $\rho_m(x)$ is local matter density at location x . This has been largely validated in more modern simulations that feature detailed feedback models (see, e.g., Martizzi et al. 2019, Walker et al. 2024). This linear scaling of $n_e(x)$ allows DM_{IGM} to be calculated from the matter density field of non-hydrodynamical N -body simulations (e.g. Pol et al., 2019; Lee et al., 2022) or density reconstructions from galaxy redshift surveys (Simha et al., 2020; Khrykin et al., 2024a).

The first FRB-related applications of hydrodynamical simulations were by McQuinn (2014), who estimated the intrinsic variance in the extragalactic DM distribution ($p(\text{DM}_{\text{cosmic}})$; see Section 3.3), and more directly by Dolag et al. (2015) who examined the various DM contributions (analogously to Equation 3.4) in the Magnetism simulations. Since then, there have been various analyses of the FRB DM in various cosmological hydrodynamical simulations, including Illustris (Jaroszynski, 2019), IllustrisTNG (Zhang et al., 2020; Takahashi et al., 2021; Walker et al., 2024), EAGLE (Batten et al., 2021), and RAMSES (Zhu and Feng, 2021). These studies have been crucial in providing numerical predictions of the Macquart (i.e. DM-redshift) relationship, while giving insight into the possible DM_{MW} and DM_{host} contributions. An important application of the Macquart relationship derived in these simulations is to invert the DM- z relation to estimate the redshift of non-localized FRBs such as those detected in CHIME.

Most well-known cosmological hydrodynamical simulations are tuned to reproduce the observed galaxy population, such as the stellar mass function and star-formation rate densities, by regulating star-formation with supernova or AGN feedback in different ways. However, different subgrid physics models using different underlying codes can arrive at comparable results for the galaxy properties. In such cases, the diffuse gas distribution in the IGM and CGM can break the degeneracy and allow discrimination between feedback models that have similar galaxy distributions. In recent years, several cosmological simulation groups have studied the effect of varied feedback models on the cosmic baryon distribution in adequately large simulation volumes, particularly in the context of halo gas (e.g., Sorini et al., 2022; Ayromlou et al., 2023). More targeted toward FRB analysis, Khrykin et al. (2024b) studied the global cosmic baryon distribution in the SIMBA (Davé et al., 2019) simulation suite (visualized in Figure 6) decomposed into simple cosmic baryon fractions of low-density IGM (f_{IGM}) as well as the aggregate halo gas in different halo mass ranges (i.e. Equation 5). They quantified the ejection of baryons by galaxy feedback into the IGM using f_{IGM} . Without any galaxy feedback, $f_{\text{IGM}} \approx 0.60$ of all cosmic gas remain outside galaxy halos, while supernova feedback ejects some gas out of halos to increase this to $f_{\text{IGM}} \approx 0.70$. They find that some forms of AGN feedback such as thermal X-ray heating and low-velocity AGN winds increase f_{IGM} above that of supernova feedback by only a couple of percent, but

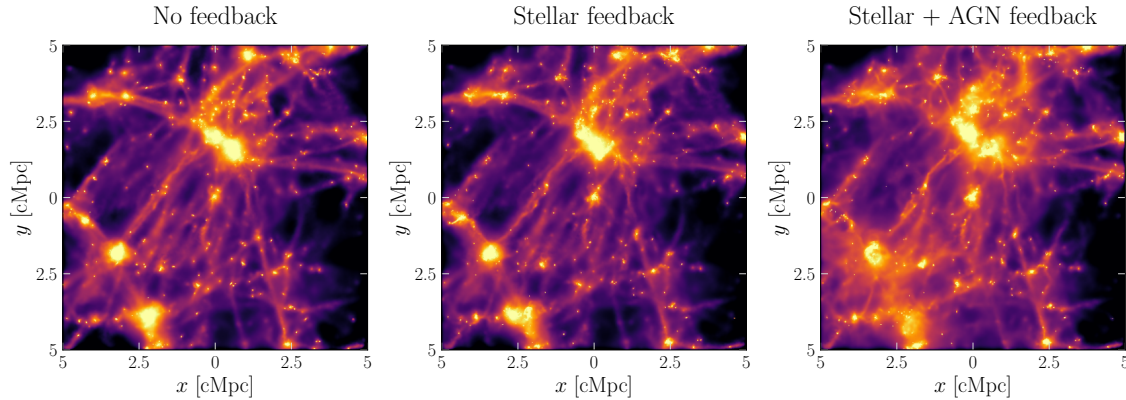


Fig. 6: Projected $z = 0$ baryon distributions from three separate runs of the SIMBA cosmological hydrodynamical simulation suite, in which different models for galaxy feedback have been applied. At left, no galaxy feedback is present, while in the middle stellar feedback from supernovae is in effect. The panel at right includes long-ranged AGN jet feedback in addition to stellar and other forms of AGN feedback. The amount of baryons residing outside of halos in these simulations is $f_{\text{IGM}} = [0.59, 0.70, 0.87]$, respectively from left to right. In all cases, the initial fluctuations that seeded the simulations were identical, but the feedback mechanisms diffuse the baryons to lower-density regions of the cosmic web to an extent apparent even by eye. Adapted from the $50 h^{-1}$ Mpc simulations in Sorini et al. (2022), with f_{IGM} values from Khrykin et al. (2024b). Credit: Daniele Sorini.

bipolar jets driven by inefficiently-accreting AGN can efficiently eject baryons out of galactic halos, such that as much as $f_{\text{IGM}} \approx 0.87$ of the cosmic baryons reside in the low-density cosmic web. Given that a FLIMFLAM-like experiment with a sample of ~ 100 localized FRBs is forecasted to a precision of $\sigma(f_{\text{IGM}}) \approx 0.06$ (Lee et al., 2022), we expect at least $3 - 4 \sigma$ constraints on the nature of AGN feedback within the next few years as such data sets become available. These constraints will be even tighter when combined with measurements of the gas mass fraction from the FRB DM_{halos} (see Section 4.2).

Meanwhile, ‘zoom-in’ hydrodynamical simulations such as the FIRE or Auriga suites simulate individual galaxies at much finer resolution than feasible with cosmological hydrodynamical simulations. These yield detailed insights into the nature of the CGM halo gas, but the statistical samples from zoom-in simulations are too small to yield statistical predictions suitable for DM_{halos} analysis in FRBs. They have, however, been crucial in providing physical insight into halo CGM gas (see Section 4.2). One promising avenue where zoom-in simulations can contribute to FRB analysis is regarding the host contribution (DM_{host}) (e.g. Orr et al., 2024). This is because DM_{host} includes contributions from their immediate FRB progenitor environments, possibly embedded within the gaseous nebulae or ISM of the host galaxy. Detailed ray-tracing analysis from large numbers of random positions drawn from even a small number of ‘zoom-in’ simulations can potentially shed light onto the DM_{host} distribution, especially in combination with observational samples of precisely-localized FRBs that can be associated to specific locations within their host galaxies (e.g., Mannings et al., 2021; Gordon et al., 2023). If strong physical priors can be built for the DM_{host} of individual galaxies, it would in turn allow tighter constraints on DM_{IGM} and DM_{halos} (c.f. Equation 7).

To-date, most large-volume (box sizes of $L \sim O(100 \text{ Mpc})$) cosmological hydrodynamical simulations have been run with just a single set of subgrid physics models due to the computational cost, or at most with a small set of model variations (Sorini et al., 2022; Ayromlou et al., 2023; Schaye et al., 2023). Each simulation suite therefore provides just a limited number of fixed models for comparison with FRB (or any other) observations. The CAMELS simulation suite (Villaescusa-Navarro et al., 2021), however, point to an intriguing new possibility: these are suites of hydrodynamical simulations where a small set of cosmological and galaxy feedback parameters, θ , are varied over ~ 1000 simulation boxes. In principle, these can be used to train parametric forward models of mock observables using machine-learning techniques, which can in turn be used to analyze real observations to constrain the best-fit θ in the real Universe. At the moment, however, the small box sizes in CAMELS ($L = 25 h^{-1} \text{ Mpc}$) do not capture statistically representative volumes of the Universe and therefore should not be used for comparisons with observational data, but future iterations could be more useful for observational analysis. Nevertheless, they are useful to study qualitative trends and gain insight: Medlock et al. (2024) used CAMELS to elucidate the trend of the FRB DM contributions from CGM in lower-mass halos.

4.2 Studying Halo Gas

The extended overdensities comprising galaxy halos extend far beyond the visible stellar and gas components usually considered to be the galaxies themselves. For example, the radius of the Milky Way disk is approximately 15 kpc based on its visible stellar distribution, but its halo has a virial radius of 240 kpc (Kaffe et al., 2014) which is enveloped by the gaseous CGM in addition to the underlying dark matter. In the literature, the CGM, Intra-Group medium (IGrM, to differentiate it from the IGM), and the intra-cluster medium (ICM) are terms referring to circum-halo gas with the approximate halo mass ranges $M_h \lesssim 10^{13} M_{\odot}$, $10^{13} M_{\odot} \lesssim M_h \lesssim 10^{14} M_{\odot}$, and $M_h \gtrsim 10^{14} M_{\odot}$, respectively. Historically, the ICM has been the most intensely-studied since it is hot enough to be observed as X-ray emission, and more recently through the thermal Sunyaev-Zel’dovich (tSZ) spectral shift imprinted on the background CMB signal. On the other hand, the CGM of $M_h \lesssim 10^{13} M_{\odot}$ galaxies have not historically been detectable in the X-ray and tSZ, but new data from the all-sky eROSITA X-ray telescope

is beginning to allow stacked X-ray analyses (Chadayammuri et al., 2022). Instead, for the lower-mass CGM, UV absorption lines observed from space have been the requisite probe in the past two decades. This includes absorption from hydrogen Lyman- α as well as a plethora of metal ionization lines, including NaI, MgII, CIV, CII (Tumlinson et al., 2017). While tremendous progress has been made especially since the advent of the UV-sensitive Cosmic Origins Spectrograph (COS) on the Hubble Space Telescope, the interpretation of these absorption lines are challenging. Modeling these absorbers require various assumptions on the metallicity, temperature, density, turbulence, ionizing flux, and properties. These analyses typically use the classic CLOUDY photoionization modeling code which make several simplifying assumptions such as chemical equilibrium and simple absorber geometries. These complications impact various analyses of the CGM, including relatively basic properties such as their radial profiles and contribution to the cosmic baryon budget.

FRBs, of course, open up the study of the CGM due to the comparatively simple assumption required in DM analysis that the gas be ionized, with the caveat that the DM is an integral measure of all the ionized gas along the FRB sightline. From among the first samples of localized FRBs, Prochaska et al. (2019) discovered that FRB20181112, with a host redshift of $z = 0.4755$, has a foreground galaxy at an impact parameter (i.e. transverse separation) of 5 arcseconds. At the foreground redshift of $z = 0.3674$, this translated to a physical separation of just 29 kpc, i.e. well within the virial radius of the intersected galaxy, which has a relatively high stellar mass of $\log_{10}(M_*/M_\odot) = 10.7$. The halo CGM contribution from this galaxy was estimated at $\text{DM}_{\text{halo}} \approx 50 - 120 \text{ pc cm}^{-3}$, i.e. a small fraction out of the overall $\text{DM} = 589 \text{ pc cm}^{-3}$ measured from the FRB. The large range in DM_{halo} illustrates the main challenge of using FRBs for studying the CGM, which is that only a small number of foreground halos are intersected per sightline on average (Ravi, 2019; Lee et al., 2022; Walker et al., 2024) with sub-dominant contributions to the overall FRB DM, so ensembles of FRBs are required in order to study the halo DM contribution. As discussed in Section 3.4, it would be easier to separate out the DM_{halos} contribution when detailed spectroscopic data is available for the FRB foreground, but cross-correlation measurements of sufficiently large numbers of FRBs with photometric redshift data might also be used to study the CGM in the future.

In order to compute the theoretical DM_{halos} contribution, assumptions need to be made regarding the gas radial profile of the CGM, as well as the normalization for each halo. The most commonly-adopted profile is the modified Navarro-Frenk-White (mNFW) profile by (Prochaska and Zheng, 2019), where the baryon density at radius r given by:

$$\rho_{\text{gas}} = \frac{\rho_{\text{gas}}^0}{y^{1-\alpha}(y_0 + y)^{2+\alpha}}, \quad (8)$$

where ρ_{gas}^0 is the central density, and $y \equiv c(r/r_{200})$ is the radius rescaled by the halo concentration parameter c and normalized by r_{200} , the characteristic radius at which the halo density is at $200\times$ that of the cosmic critical density. The profile parameters α and y_0 are typically set to $\alpha = 2$ and $y_0 = 2$. This choice of parameters is designed to mimic gas profiles in the multi-phase CGM (Maller and Bullock, 2004). However, there is a lively ongoing debate on the detailed astrophysics governing the CGM of Milky Way-like and lower-mass galaxies ($M_h < 10^{12.5} M_\odot$), where competing effects such as hot gas pressure, cold-flow accretion, turbulence, and cold gas precipitation could alter the halo gas profiles. The radial ionized gas profiles are thus in fact model-dependent and give specific predictions for the FRB DM_{halos} (e.g., Stern et al., 2019; Singh et al., 2024), but it would likely require future samples of hundreds of localized FRBs to achieve sufficient sensitivity to differentiate between different radial profiles. The mNFW profile is therefore a useful ansatz to use in the meantime.

Following conventions first established by the galaxy cluster community, for a given halo with mass M_h , one can then define the gas fraction $f_{\text{gas}} \equiv M_{\text{gas}}/(\Omega_b M_h)$, which is relative to the amount of baryons available within the halo if baryons simply traced the halo dark matter by the cosmic baryon fraction. This sets the per-halo normalization ρ_{gas}^0 in Equation 8. The DM_{halo} for a given galaxy or halo is then simply the path integral of Equation 8, assuming that all the baryons are ionized, along the chord though the halo at the appropriate impact parameter. Since only the aggregate DM is measured for a given FRB, the $\text{DM}_{\text{halos}} = \sum_i \text{DM}_{\text{halo},i}$ contribution along the lines-of-sight typically needs to be modeled statistically from the FRB population, or alternatively through individual lines-of-sight if data were available for the FRB foreground fields (see text box “Impact of Photometric vs Spectroscopic Redshifts on the FRB DM” below).

The most straightforward approximation is to adopt a single value of f_{gas} across the entire mass range of intersected foreground halos, but the behavior of f_{gas} across different halo masses is actually an open question. The deep gravitational wells in massive $M_h \gtrsim 10^{14} M_\odot$ galaxy cluster halos — and observational constraints through X-ray emission and the thermal Sunyaev-Zel’dovich effect — lead to a consensus for a relatively large $f_{\text{gas}} \sim 0.7 - 0.9$ for clusters (e.g., Mantz et al., 2014; Eckert et al., 2022). In other words, there are few feedback mechanisms that can eject baryons entirely out of cluster halos, and once all the gas and stars within a cluster boundary are considered, they are usually consistent with the cosmic baryon fraction Ω_b/Ω_m (Rasheed et al., 2011). In lower-mass halos ($M_h \lesssim 10^{14} M_\odot$), the competing and interconnected effects of supernovae as well as various forms of AGN feedback embedded in shallower gravitational potentials typically lead to lower f_{gas} , but there is little theoretical consensus as to the trend with mass from different simulations (Figure 7). Future FRB observations of DM_{halos} covering a wide range of galaxy halo masses can therefore be valuable in measuring this trend with mass, especially at lower masses ($M_h \lesssim 10^{13} M_\odot$) that are challenging to probe by other observational techniques (c.f. observational data points in Figure 7).

Impact of Photometric vs Spectroscopic Redshifts on the FRB DM

In extragalactic astronomy, the redshift of a galaxy is typically the best proxy for its distance by using the Hubble distance-redshift relation. Spectroscopy allows galaxy redshift to be measured to an accuracy of $\sigma_z/(1+z) \sim 10^{-3} - 10^{-4}$ by comparing the observed wavelength of spectral features to their restframe values, but is traditionally time-consuming compared to imaging observations. On the other hand, imaging sky surveys using multiple broadband filters such as Pan-STARRS, DES or DECaLS, and Subaru HSC can cover many more objects over far greater sky areas. The galaxy fluxes observed in different imaging filters can

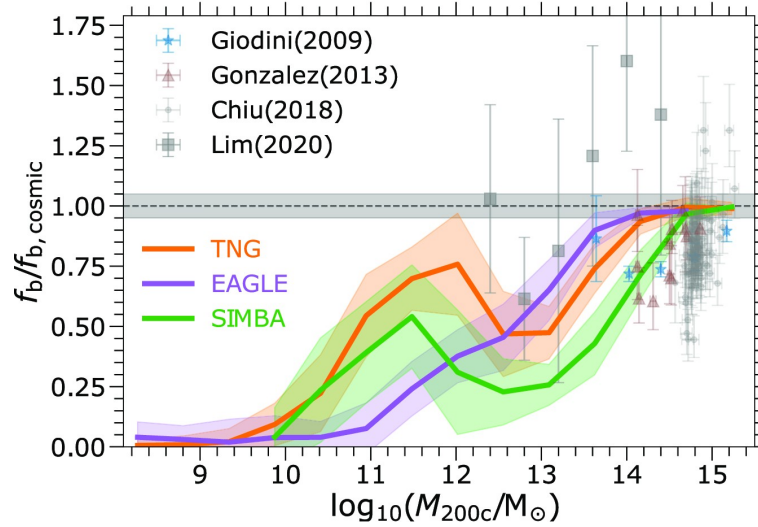


Fig. 7: The baryon fraction, f_b , within halos relative to the cosmic baryon fraction, Ω_b/Ω_m , as a function of halo mass in several cosmological hydrodynamical simulations (colored lines, where the shaded regions indicate the scatter within the simulation). In this figure, f_b includes contributions from stars, ISM, and halo gas, but since the latter is the dominant component a lot of the trends are driven by it. The error bars indicate observational constraints from various techniques. For halos with $M_h \gtrsim 10^{14} M_\odot$, f_b trends toward the cosmic value, but the different simulations disagree for galaxy- and group-sized halos. Excerpted from Ayromlou et al. (2023) (Credit: Reza Ayromlou).

be used to estimate photometric redshifts by comparing with spectral template libraries, but with significant errors. For example, the Dark Energy Survey reports $\sigma_z \approx 0.1$ at $z = 0.25$, i.e. for a galaxy at this redshift the 1-sigma photometric redshift uncertainties will bracket $z = 0.15$ and $z = 0.35$. For calculating DM_{halo} contributions, the largest effect of this uncertainty is in changing the assumed intrinsic luminosity (and hence stellar and halo mass) of the foreground galaxies. As a worked example, a $z = 0.25$ galaxy with a Milky Way-like stellar mass of $M_*/M_\odot = 10^{10.6}$ (corresponding to a halo mass of $M_h/M_\odot \approx 10^{12.1}$) separated by 20 arcseconds from a hypothetical FRB sightline would contribute $\text{DM}_{\text{halo}} = 36 \text{ pc cm}^{-3}$ assuming the mNFW radial profile and $f_{\text{gas}} = 0.5$ (see Section 4.2). Since the apparent luminosity does not change, the aforementioned 1-sigma bounds of $z = 0.15$ and $z = 0.35$ would modify the implied stellar mass by the change in distance modulus $\Delta\mu$ ($M_* \propto 10^{-0.4\Delta\mu}$ and assuming stellar mass is traced by luminosity), the resulting 1-sigma uncertainty in the foreground DM contribution would span $\text{DM}_{\text{halo}} = [24, 85] \text{ pc cm}^{-3}$. For lower-redshift FRBs, these errors (as well as a 5–10% possibility of >2-sigma ‘catastrophic’ redshift errors) can additionally lead to uncertainties as to whether a galaxy is in the foreground or background in the first place. Therefore, while photometric redshifts can come for ‘free’ in pre-existing wide-field imaging surveys such as Pan-STARRS or DES, much larger samples of FRBs are required to overcome the uncertainties introduced by photometric redshifts. Reconstructing the cosmic web, like in Figure 5, would moreover be unfeasible.

The overall contribution of the halo gas to the cosmic baryon budget, f_{cgm} (see Equation 5), can generally be calculated by integrating over the halo mass function $\phi(M_h)$:

$$f_{\text{cgm}} = \frac{\int_{M_1}^{M_2} [\rho_{\text{gas}}(r) 4\pi r^2 dr] \phi(M_h) d \ln \frac{M_h}{M_\odot}}{(\Omega_b/V) \int_V \bar{\rho}_m(z) dV}. \quad (9)$$

Typically, this integral is evaluated to $r_{\text{max}} = r_{200}$, although how to exactly model the IGM-CGM boundary is still an open question. In many previous FRB analyses (Lee et al., 2022; Khrykin et al., 2024a), the integrated mass range $[M_1, M_2]$ spanned the full range of non-cluster halos $10^{10} \lesssim M_h/M_\odot \lesssim 10^{14}$. This implicitly assumes a fixed f_{gas} over this entire mass range, which is probably incorrect according to studies of halo gas in hydrodynamical simulations (Figure 7). A more general treatment would allow a mass-dependency of f_{gas} , or alternatively to split the mass ranges for the integral over which f_{gas} is expected to be relatively stable and then split their cosmic baryon contributions (e.g. Equation 5).

As FRBs are detected at increasing redshifts ($z \sim 1$ and beyond), they will begin probing the epoch at which the photo-ionized Lyman- α forest at $z \gtrsim 2$ evolves into the WHIM and CGM observed at low redshifts ($z < 1$). One might then expect a redshift evolution in f_{gas} as a function of halo mass, as well as f_{IGM} .

4.3 Impact on Weak-Lensing Cosmology

The relative distribution of baryons across the Universe has consequences for cosmological analyses, especially those using gravitational lensing or galaxy clustering. The ratio of baryons to dark matter ($\sim 1 : 5$) is large enough that a more diffuse distribution of cosmic baryons, such as that caused by AGN jet feedback (the right panel of Figure 6), would smooth out the overall matter field compared to a purely CDM Universe.

Many cosmological analyses aim, directly or indirectly, to measure the matter power spectrum $P(k)$, which codifies the fluctuations of

large-scale structure on various scales corresponding to Fourier wavenumber k (as a rough approximation, the corresponding real-space scale is $L \sim 1/k$). The behaviour of baryons can therefore lead to biased cosmological analyses due to so-called ‘baryonic effects’ that modify the matter power spectrum, beyond that computed from collisionless CDM alone. Various cosmological hydrodynamical simulations have different predictions for these baryonic effects, usually parametrised by the ratio of the power spectrum in the hydrodynamical simulation compared with that calculated from CDM alone, $P_{\text{hydro}}(k)/P_{\text{cdm}}(k)$. This is one of the possible solutions to the so-called S_8 tension, which is the discrepancy in the level of matter fluctuations, $S_8 \equiv f \sigma_8$, detected in the low-redshift Universe when compared with the precise value inferred from the CMB in early times.

Most observational constraints that aim to constrain these ‘baryonic effects’ have focused on f_{gas} measurements in halos using X-ray or Sunyaev-Zel’dovich measurements, especially in galaxy group-sized halos ($M_h/M_\odot \sim 10^{13}$) where feedback can potentially eject significant amounts of baryons out to large scales. FRB measurements, uniquely, can measure f_{IGM} , which is the destination of the ejected gas, while also measuring f_{gas} across a range of halo masses. This should place independent constraints on the effect of baryonic effects in cosmology.

5 The Hubble tension

The cosmic expansion rate of the Universe, $\dot{a}(t)$, describes the fact that galaxies are moving away from each other proportional to their distance. The velocity of these galaxies relative to Earth was determined by their redshift, and this work is attributed to Edwin Hubble - Hubble’s Law (Hubble, 1929), although the idea that the Universe was expanding was previously derived through general relativity by Friedmann (1922), and measured observationally (e.g. Wirtz, 1922). The linear relationship between recessional velocity v and the proper distance D between galaxies is parametrized by $v = H_0 D$; ergo, H_0 characterizes the expansion rate of the Universe at the present time. At redshift $z = 0$, the Hubble parameter can be described as $H(z) = \dot{a}(t)/a(t) = H_0 \sqrt{\Omega_\Lambda + \Omega_m(1+z)^3}$, where Ω_Λ is the vacuum energy density fraction, and Ω_m is the matter density fraction. Furthermore, while a non-zero ‘deceleration parameter’ implies either a slowing expansion due to gravitational attraction, or an accelerating one (as currently believed), current estimates of the age of the Universe are close to the Hubble age, defined as $t_H = 1/H_0 \sim 14.4$ billion years. As the age and expansion of the Universe is a key feature of its history, H_0 underpins the various models that have been developed to describe the evolution of the Universe.

The measurement by Edwin Hubble in 1929 of the Hubble constant was $500 \text{ km s}^{-1} \text{ Mpc}^{-1}$, which was achieved by studying bright stars in galaxies. This value is far larger than those values that are currently adopted in cosmology. We say values in plural form, because there have been numerous measurements of H_0 since, arising from all sorts of methodologies. Two notable general measurement methods exist; one is the ‘distance ladder’ or ‘late Universe’ case, which relies upon accurate distance measurements in nearby galaxies, and then using so-called standard candles, e.g. type 1a supernova, as milepost markers to much more distant galaxies. The other is to measure the cosmic microwave background (CMB) - also termed as ‘indirect’ or ‘early Universe’ measurements of Hubble’s constant.

Crucially, these two methods do *not* agree with each other. The commonly accepted value of $H_0 = 73.04 \pm 1.04 \text{ km s}^{-1} \text{ Mpc}^{-1}$ (Riess et al., 2022) from local type 1a supernova is in tension by $\sim 4\sigma$ with Planck observations of the CMB: $H_0 = 67.4 \pm 0.5 \text{ km s}^{-1} \text{ Mpc}^{-1}$ (Planck Collaboration et al., 2020). This is described as the Hubble tension, and has been viewed as either a ‘crisis for cosmology’ (our theories on the Universe are incomplete and need correction to reconcile this difference), or an indication that our measurements hold some flaw and require a correction (e.g. we are missing an observational effect), and/or better datasets. Figure 8 visually highlights the Hubble tension from observations across the literature (Di Valentino et al., 2021).

While both sides aim to resolve this, alternative approaches may be able to weigh in on the matter.

5.1 FRBs as another probe of the Hubble Constant

FRBs are one such pathway to investigate the Hubble tension. While as previously described the majority of fast radio bursts are as yet unlocalized, the number of FRB host galaxies that have been identified and with spectroscopic redshift measurement has been ramping up. The cosmic contribution to the DM probed by an FRB along its line of sight ($\text{DM}_{\text{cosmic}}$) is key; the average value of $\text{DM}_{\text{cosmic}}$ is proportional to both the baryon fraction Ω_b and H_0 . As $\Omega_b H_0^2$ is measured through the CMB, the average $\text{DM}_{\text{cosmic}}$ value is hence proportional to H_0^{-1} . With a sufficient number of FRBs with a good spectroscopic redshift (and hence distance) measurement, and a proper understanding of the distribution of ionized electrons contributing to the DM measured by each source, one can independently test for a value of the Hubble constant, up to the redshift distribution of FRBs.

There have been a few preliminary studies either observationally or with simulated FRBs. James et al. (2022) demonstrated the ability to place a wide constraint on the Hubble constant, arriving at $73_{-8}^{+12} \text{ km s}^{-1} \text{ Mpc}^{-1}$ with a sample of 16 localized and 60 unlocalized FRBs - a value currently consistent with both direct and indirect measures of H_0 . A key aspect of this work was the use of uniform priors across several parameters (i.e. systematic uncertainties which need to be properly accounted for), including the DM contribution from the host galaxy. James et al. (2022) also predicted through Monte Carlo simulations that 100 well-localized FRBs will be able to constrain H_0 with a statistical uncertainty of $\sim \pm 2.45 \text{ km s}^{-1} \text{ Mpc}^{-1}$ - sufficient to break the Hubble tension to a 1σ level. We are already approaching that point. Kalita et al. (2024) recently reported a result with an error range of $\pm 2.5 \text{ km s}^{-1} \text{ Mpc}^{-1}$ with a collection of 64 localized FRBs; however to achieve this result they assumed for many FRBs in their sample a value of DM_{host} based on IllustrisTNG simulations, where a median value of $\text{DM}_{\text{host}} = 33(1 + z^{0.84} \text{ pc cm}^{-3})$ was found, as well as an estimate of DM_{halo} of $\approx 50\text{--}80 \text{ pc cm}^{-3}$. FRBs used in such studies may in the literature also have assumed values of H_0 to derive DM_{host} . While a larger sample will help further constrain the Hubble constant, a proper understanding of the amount of DM contributed by the FRB host galaxy, as well as galaxy halos, will be required to confidently claim a robust value for H_0 .

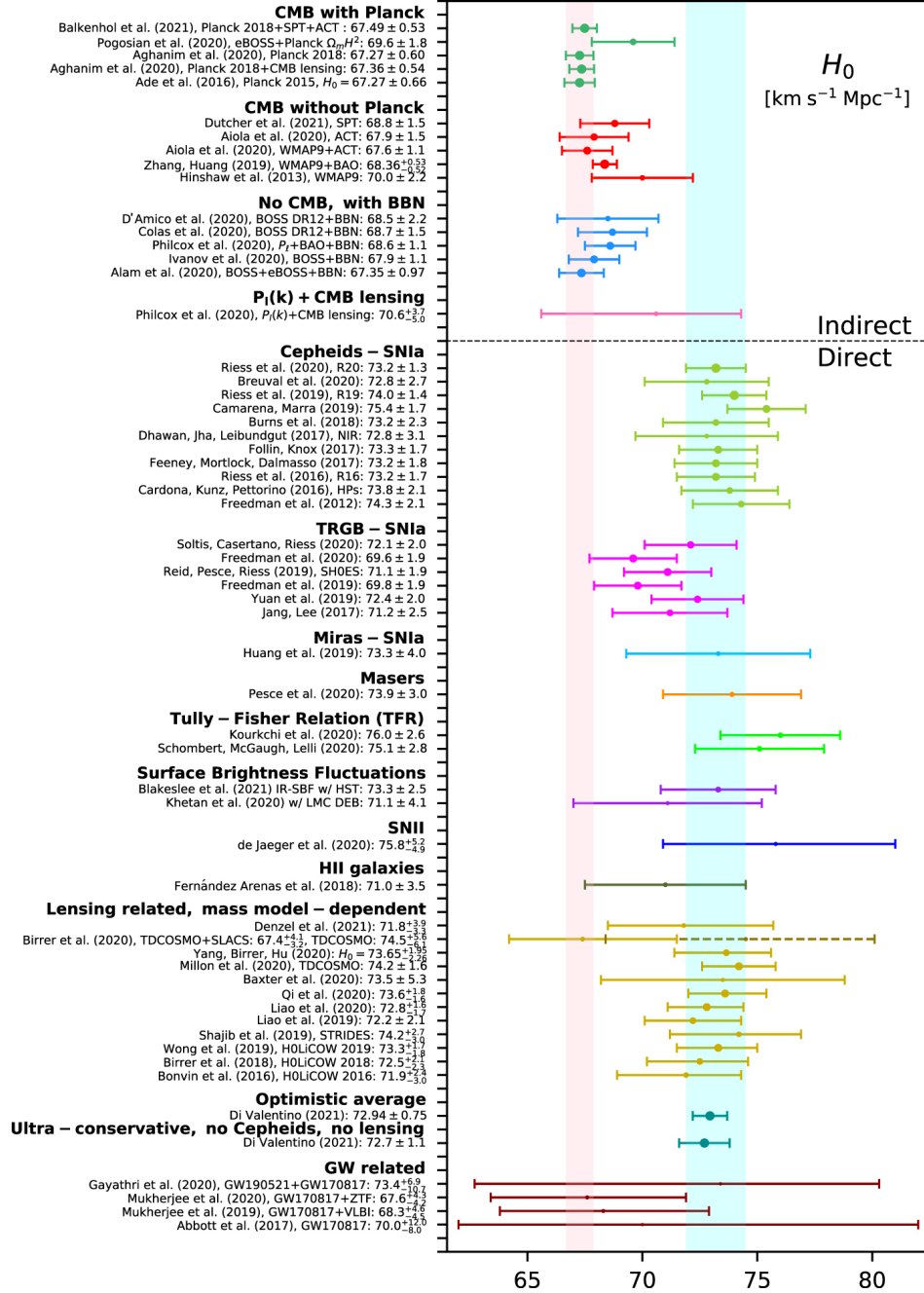


Fig. 8: Whisker plot of the 68% confidence limit (CL) constraints of the Hubble constant H_0 , through direct and indirect measurements by different astronomical missions and groups. The cyan vertical band corresponds to the H_0 value from SH0ES team and the light pink vertical band corresponds to the H_0 value as reported by the Planck experiment assuming a Λ CDM scenario. Image credit: Di Valentino et al. (2021), <https://github.com/lucavisinelli/H0TensionRealm>.

Baptista et al. (2024) also examined what the Hubble constant depended on; namely, a fluctuation parameter F ranging from 0 – 1 in value, which can be thought of as a measure of ‘clumpiness’ in the Universe (higher F values means more ‘clumps’ in large-scale structure). As one expects σ_{DM} to be proportional to $z^{-0.5}$ from the Macquart relation, one can introduce F to describe $\sigma_{DM}(\Delta) = Fz^{-0.5}$. As F increases (approaches a value of 1), the resulting spread of DM_{cosmic} increases. Baptista et al. (2024) found that F was degenerate with the Hubble constant when using FRBs from Parkes and ASKAP. Furthermore, a uniform prior on H_0 allowed a measure on F . Ergo, any investigation into H_0 also requires a careful consideration of other factors than a large sample of well-localized FRBs, but conversely FRB studies will allow us to extend such work to other important cosmological parameters. A key difficulty will be reconciling where exactly baryons are found in and outside of galaxies (Section 4).

6 Studying cosmic magnetism with rotation measure

Intergalactic magnetic fields hold various open questions, such as to their creation. Are they established shortly after the Big Bang (i.e. before the first stars and galaxies), or solely in combination with astrophysical processes such as star formation or the growth of active galactic nuclei? Perhaps the answer is a mixture? Furthermore, magnetic fields can influence star formation, and perhaps galaxy evolution, such as how spiral arms form. Studies of cosmic magnetism require radio telescopes to be able to detect polarized radiation, and to date observational constraints on cosmic magnetic fields have been scant.

The Faraday effect, or Faraday rotation, is a rotation in polarization, and is proportional to the projection of the magnetic field along the direction of the light propagation. One can measure Faraday rotation measures (RM) to probe the component of the magnetic field which is parallel to the line of sight of radio emission:

$$\text{RM} = \frac{e^3}{2\pi m_e^2 c^4} \int_z^0 \frac{n_e(z) B_{\parallel}(z)}{(1+z)^2} \frac{dr(z)}{dz} dz \text{ rad m}^{-2} \quad (10)$$

where B_{\parallel} the magnitude of the line-of-sight magnetic field. While polarized stars and pulsars have been the common astronomical sources to target for RM studies, this is largely limited to the magnetic field within our own Milky Way. FRBs offer cosmological and polarized sightlines; thus, RM studies of FRB emission can inform us on both magnetic fields within the FRB host galaxy and outer reaches of the Milky Way, and the large-scale structure (and cosmic voids) between.

Ravi et al. (2016) demonstrated the potential of RM studies of FRBs through the study of a bright, linearly polarized FRB. They found a low Faraday RM measure and inferred negligible magnetism in the circum-burst plasma, allowing a constraint on the parallel to the line-of-sight magnetic field within the cosmic web along the sightline of < 21 nG. It is noted that many other studies have often focused on RM measurements to learn about the immediate plasma environment about the FRB progenitor. Mannings et al. (2023) found a positive correlation between RM and the estimated host DM, implying the bulk of RM comes from the FRB host galaxy for 9 FRBs. RMs from zoom-in simulated Milky Way-like galaxies were also examined and found to agree with observations to within a 95% confidence interval. Significantly larger scale studies will be necessary. Zheng et al. (2014) estimated tens of thousands of FRBs would be needed to map out the redshift evolution of RM which is caused by the IGM magnetic field. Kovacs et al. (2024) extended the simulation approach with 16,500 galaxies from the IllustrisTNG50 simulations, and made predictions for the number of FRBs required to detect the intergalactic magnetic field for given measures of the standard deviation $\sigma_{\text{RM,IGM}}$ - a value of 2 rad m^{-2} would require $\sim 95,000$ FRBs at $z = 0.5$, or $\sim 9,500$ FRBs at $z = 2$.

7 Scattering

There are two other notable effects that can be observed in the frequency vs. time figures of fast radio bursts. One is a temporal broadening of the pulse, typically as an exponential tail in the profile, which is called scattering, which we focus on here. Scattering is due to multi-path propagation through inhomogeneous media - fluctuations in the electron density medium through which FRB signals propagate can alter the path FRBs take to an observer. This multi-path propagation effect, similarly, is responsible for scintillation, which is seen in the frequency domain. As with DM, the contributors to these effects include the Milky Way and the FRB host galaxy. The immediate environment around the FRB progenitor could also be largely responsible, particularly if it is embedded in a highly magnetised plasma - fitting if at least some FRB progenitors prove to be magnetars. Ocker et al. (2022) reported for the repeating fast radio burst FRB 20190520B that both the bulk of the DM and observed scattering was dominated by the host galaxy, although intervening galaxies could also contribute significantly to scattering for other FRBs. Such studies with FRBs are crucial for investigations into plasma screens and turbulence within galaxies, and may be key for testing FRB progenitor models.

Scattered FRBs offer another way to aid investigations into disentangling the contributors to DM, as well as identifying large-scale structure along the FRB line of sight. Individual FRBs can be significant for such studies in themselves. Shin et al. (2024) presented an extreme example: FRB 20200723B, with a scattering timescale of over 1 second (typical scattering timescales are \sim milliseconds) at 400 MHz, coupled with a relatively low DM of $\sim 244 \text{ pc cm}^{-3}$. Due to its location to a sheet filamentary structure near the Virgo Cluster, an upper limit could be placed on the average free electron density on the structure, allowing for a comparison to cosmological simulations. Such studies can also be extended with an ensemble of scattered FRBs, even if they do not offer such extreme and useful ‘conditions’ (e.g. high scattering times) individually. Connor et al. (2024) considered a sample of over 60 well-localized FRBs, including three FRBs near or beyond a redshift of $z = 1$, where scattering properties were used to aid constraints on individual contributions of DM for each sightline.

One drawback with scattering studies is that this can hamper the ability to detect the FRB, particularly at lower frequencies. Assuming a fixed bandwidth, as the frequencies at the edges of the bandwidth decrease, the time delay between photons at those frequencies will increase (Equation 1). Scattering further widens the dispersed pulse and can decrease the signal strength, reducing the chance of detection. Lower time resolution searches is also a factor to consider, as the quantitative amount of scattering (often described as τ) will be harder or impossible to determine. Increasing the time resolution is an option, albeit an expensive one in regards to data rates and storage. An ability to beamform FRB data, as demonstrated with the ASKAP and MeerKAT telescopes for instance, allows one to obtain high-time resolution polarimetric datasets of FRB emission, but requires a mechanism to do voltage dumps upon real-time detection and then reduction of that data. Furthermore, without high-time resolution datasets and a high signal-to-noise detection, making fits to the pulse in order to derive a scattering timescale is difficult, and may only be able to render an upper limit. This is less of an issue with larger FRB datasets, but again

effective localization of the FRB is required to maximise analysis regarding scattering and DM measurements. Such samples will lead to further potential studies, such as an examination of if scattering measures are correlated with either global galaxy properties, or the local region around the FRB for cases where the FRB can be localized to a small region within their host galaxy. The former can help determine if, for a majority of scattered FRBs, whether the amount of scatter is indeed largely due to the host galaxy, and what constraints can be then placed on the IGM, while the latter informs on the local environment around the progenitor, and potential plasma screens and associated magnetic fields.

8 Further cosmology questions

In addition to the previous topics, FRBs may aid our investigations into further areas of cosmological research, some which we briefly summarise.

8.1 Shapiro time delay

The Shapiro time delay effect, also described as gravitational time delay effect, is a classic test of general relativity and Einstein’s weak equivalence principle, which was conducted within the Solar system. First proposed by Shapiro (1964), the idea is based on the fact that the speed of a light wave depends on the strength of the gravitational potential along its path. Shapiro predicted measurable time delays to be seen for path lengths close to the Sun (accounting for a path length increase of ~ 60 km). Radar tests a few years later were able to verify Shapiro’s calculations, and have been repeated since with further success.

This effect can be extended beyond the Solar system, and fast radio bursts are excellent probes of this across cosmological distances. Hashimoto et al. (2021b) investigated this with two repeating FRBs, and from testing the time lag between photons with different energies through observational uncertainties of the DM measured for those FRBs, derived constraints comparable to the tightest made through other methods. A much larger population may further extend current constraints. Wucknitz et al. (2021) also demonstrated an exciting prospect should an ensemble of gravitationally lensed repeating FRBs be identified; through a mock sample of simulated lenses, strong constraints on cosmological parameters can be made, which requires a measurement of the Shapiro delay in relation to the lens system.

8.2 Cosmic reionization

The Epoch of Reionization is the period where neutral hydrogen in the Universe reionized. Prior to this event, the Universe was relatively opaque at absorbed wavelengths of $\lambda < 911$ nm, and transparent otherwise. Once gas clouds started to condense and began forming the first stars (although other candidates for the source of reionization exist such as dwarf galaxies), the radiated ionizing flux converted the largely neutral atomic content into ionized plasma. Many questions remain as the Epoch of Reionization is yet to be directly observed, and so when it began, as well as the fraction of ionization, still under investigation through observational studies of Lyman alpha and the neutral hydrogen 21-cm line in emission, and of the power spectrum measured from the cosmic microwave background polarization. This is a crucial part of the Universe’s history to try to understand, and the focus of many new and upcoming telescopes.

The IGM dispersion measure derived from detected FRBs is an indicator of the amount of ionized material in the IGM, and is proportional to the ionization fraction. Hashimoto et al. (2021a) demonstrated a proof of concept by constructing mock non-repeating FRBs to be detected with the upcoming SKA radio telescope. This study was able to reconstruct reionization histories from this mock FRB data, providing another potential avenue for exploring the Epoch of Reionization with new radio telescopes. Heimersheim et al. (2022) considered the optical depth of the cosmic microwave background and found that it could be independently constrained with 100 localized FRBs, between redshifts of $5 < z < 15$ to within 11%, and the midpoint of the Epoch of Reionisation to 4% accuracy. These forecasts, naturally, assume that FRBs — whatever they may be — can occur at very high redshifts.

8.3 Photon mass limits

While photons are considered to be massless as a consequence of e.g. Maxwell’s equations and Einstein’s theory of special relativity, the nature of physics research and theory demands experimental study to confirm such conclusions, or otherwise attempt to disprove them. If a non-zero mass is discovered for photons, then a rethink of these fundamental equations and theories would be required. Experimental tests for photon mass typically aim to measure the time delay induced by speed reductions below the standard speed of light, that a finite photon mass would induce. To date only upper bounds have been obtained through measurements of flare stars, timing of the Crab Nebular pulsar, and gamma-ray bursts. The time delay of FRBs are yet another potential tool to further constrain the photon mass. Both Bonetti et al. (2016) and Wu et al. (2016) independently used FRB 20150418A to place an upper limit upon the photon mass (3.2×10^{-50} kg and 5.2×10^{-50} kg respectively), a factor of $\sim 1000\times$ improvement on limits obtained from other astrophysical sources. Further redshift measurements of distant FRBs will enable even further constraints on the photon mass. However, since the primary time delay in FRBs is induced via plasma dispersion from cosmic baryons, the latter would need to be understood with high confidence.

9 Enabling future FRB-driven studies into cosmological mysteries

In order to best enable our ability to answer the above outstanding questions for cosmology through FRBs, further progress is required across astronomy research. A key area is based upon the radio observations themselves: the detection and high-quality localization of

many more FRBs. We wish to probe cosmological distances and hence the large-scale structure of the Universe in order to determine the underlying parameters that govern the cosmos we find ourselves in, as well as study sightlines through our own Milky Way and its halo which enables constraints to be placed on CGM models. To achieve this, accurate redshift measurements are required for a much larger sample than what we currently have. Underpinning that goal then are the radio telescopes. We are already in the midst of a great age of radio astronomy, and this applies to the field of FRB research. ASKAP, CHIME, DSA-100, FAST, MeerKAT, and Parkes are the current leading drivers of FRB detection, with three of these also capable of localizing the majority of their detected FRBs to their host galaxies. CHIME outriggers actively being commissioned will also ensure localization for many of the FRBs detected by that telescope. FAST will expand into the FAST Core Array, which will feature 24 new 40 m diameter movable radio telescopes, and grant an angular resolution of 4.3", sufficient for localizing more nearby FRBs to their host galaxies (Jiang et al., 2024).

Meanwhile, several more radio telescopes are under development. The Bustling Universe Radio Survey Telescope in Taiwan (BURSTT; Lin et al., 2022) will have all-sky coverage across 400 MHz bandwidth coupled with sub-arcsecond localization through its own outrigger stations. DSA-110 is aiming to upgrade to DSA-2000¹, and will potentially detect and simultaneously localize $\sim 10,000$ FRBs each year. The SKA is projected to detect $\sim 10,000$ non-repeating FRBs at redshift $z \sim 2$ per year, and 10 at redshift $z \sim 6$ per year (Hashimoto et al., 2020). Zhang et al. (2023) finds that with the SKA alone, when simulating such numbers of localized FRBs, that the dark-energy equation of state parameters can be tightly constrained, and the baryon density measured to a precision of 0.1%. And the Very Large Array is set to be expanded into the Next Generation Very Large Array (ngVLA), which will operate at a higher frequency regime than aforementioned telescopes (the lower band of two on the ngVLA receives are to span the frequency range of 1.2–50.5 GHz). These are just some of the current projected telescopes: other yet-unrealized concepts, that would be significantly cheaper than others to produce, could still make significant contributions to this space. An example is the Compact All-Sky Phased Array (CASPAs; Luo et al., 2024), which would be optimal for detecting FRBs in the nearby Universe and for extending the high-end of the FRB luminosity function while surveying the entire Southern sky, and for example also shadow gravitational-wave observations.

To properly realize these upcoming telescopes, they would need to be supported via their backend systems. The ability to enable FRB science with methods for real-time detection, and voltage capture which necessitates large storage space will be important. So too will the compute requirements - both in space and reliability - for reducing and then analyzing the radio telescope data, which has already been a concern for current generation telescopes. And of course, personnel must not be forgotten either, on both the astronomy and engineering side, to develop, maintain, and analyze the technology and surveys, such as in the development of novel detection and reduction algorithms. As described in Section 1, the discovery of the first FRB arose from the creation of a single-pulse search code. The CRAFT Effortless localization and Enhanced Burst Inspection Pipeline (CELEBI; Scott et al., 2023) is an example of a complex pipeline for turning radio voltage data into FRB localizations. CELEBI was prepared for the CRAFT COherent upgrade (CRACO; Wang et al., accepted), a coherent search system that will detect $10\times$ the FRBs to previous CRAFT work. Such new FRB search and data reduction systems will need to be perfected, lest astronomers figuratively drown in high FRB detection data rates.

Follow-up of radio localizations of FRBs is then essential. While one can use H_i detected through the 21-cm transition to determine a redshift for the FRB host galaxy (Glowacki et al., 2024), this is only useful in a subset of FRB hosts in practice: said galaxies require sufficient amounts of neutral hydrogen gas, even if we tend to find FRBs in gas-rich star forming galaxies. Not all telescope FRB searches are in spectral line mode. Furthermore, the 21-cm transition is currently difficult to detect beyond redshifts of $z > 0.1$ due to a redshift-dependent $((1+z)^{-4})$ surface brightness dimming, without extensive observing time with even the most sensitive radio telescopes currently in operation. In most cases, optical follow-up is a must. It is noted that it may be viewed that the more FRBs that are detected and localized, the less interesting obtaining ‘yet another redshift’ will become to the wider community, even though cosmological studies with FRBs demands ensembles of spectroscopic redshift measurements of their host galaxies. We may in the longer term rely on archival redshifts from either current surveys, such as the Sloan Digital Sky Survey (SDSS), which spans the northern sky but only with good spectroscopic redshift coverage at lower redshifts ($z \lesssim 0.15$), or next-generation ones such as the DESI Bright Galaxy Survey which pushes SDSS-like spectroscopic completeness to $z \sim 0.3$, also in the north. This redshift range is already coming up short with regards to the increasing samples of high-redshift FRBs, and of little help to FRBs localized in the southern skies. The 4-metre Multi-Object Spectroscopic Telescope (4MOST; de Jong et al., 2019) will offer spectroscopic coverage of a significant area of the Southern Sky - but is yet to start operation at the time of writing. Still, there will be some avenue where follow-up may be less necessary for FRBs sans the most extreme (and hence interesting and potentially most useful for addressing these science goals), in a space where applying for telescope time is already fiercely competitive (the James Webb Space Telescope for example has had over-subscription rates of 4.1–9:1).

The ability to couple these observational studies with our theories of the Universe will also be crucial. Hydrodynamical and cosmological simulations have already been essential tools in other areas of cosmology research, and offer levels of precision in measurement not possible with current observations. As our FRB surveys improve in sensitivity and scope, we will be able to further constrain both cosmological parameters and galaxy properties, and simulations offer a great testbed. It was simulations which helped inform us further on the ‘missing baryons’ problem prior to their first detection, and FRBs are a unique observation probe that can test such predictions. It goes both ways too - results from FRB observations can further constrain models to be implemented in future simulation suites.

FRBs has been a very fast moving field since their discovery within a mere two decades ago. Great steps have already been taken to get to this point, where achievements include producing the first detection of the missing baryons, placing preliminary constraints on cosmological parameters, and probing the intergalactic content of the Universe. While a lot of hard work will be required to achieve our goals, the future looks bright.

¹<https://www.deepsynoptic.org/overview>

Acknowledgments

MG is supported by the Australian Government through the Australian Research Council's Discovery Projects funding scheme (DP210102103), and through UK STFC Grant ST/Y001117/1. MG acknowledges support from the Inter-University Institute for Data Intensive Astronomy (IDIA). IDIA is a partnership of the University of Cape Town, the University of Pretoria and the University of the Western Cape. Kavli IPMU is supported by the World Premier International Research Center Initiative (WPI), MEXT, Japan. For the purpose of open access, the author has applied a Creative Commons Attribution (CC BY) licence to any Author Accepted Manuscript version arising from this submission.

References

- Ayromlou M, Nelson D and Pillepich A (2023), Oct. Feedback reshapes the baryon distribution within haloes, in halo outskirts, and beyond: the closure radius from dwarfs to massive clusters. *MNRAS* 524 (4): 5391–5410. doi:10.1093/mnras/stad2046. 2211.07659.
- Baptista J, Prochaska JX, Mannings AG, James CW, Shannon RM, Ryder SD, Deller AT, Scott DR, Glowacki M and Tejos N (2024), Apr. Measuring the Variance of the Macquart Relation in Redshift–Extragalactic Dispersion Measure Modeling. *ApJ* 965 (1), 57. doi:10.3847/1538-4357/ad2705. 2305.07022.
- Batten AJ, Duffy AR, Wijers NA, Gupta V, Flynn C, Schaye J and Ryan-Weber E (2021), Aug. The cosmic dispersion measure in the EAGLE simulations. *MNRAS* 505 (4): 5356–5369. doi:10.1093/mnras/stab1528. 2011.14547.
- Bonetti L, Ellis J, Mavromatos NE, Sakharov AS, Sarkisyan-Grinbaum EK and Spallicci ADAM (2016), Jun. Photon mass limits from fast radio bursts. *Physics Letters B* 757: 548–552. doi:10.1016/j.physletb.2016.04.035. 1602.09135.
- Cen R and Ostriker JP (1999), Jul. Cosmic Chemical Evolution. *ApJ* 519 (2): L109–L113. doi:10.1086/312123. astro-ph/9903207.
- Cen R and Ostriker JP (2006), Oct. Where Are the Baryons? II. Feedback Effects. *ApJ* 650 (2): 560–572. doi:10.1086/506505. astro-ph/0601008.
- Chadayammuri U, Bogdán Á, Oppenheimer BD, Kraft RP, Forman WR and Jones C (2022), Sep. Testing Galaxy Feedback Models with Resolved X-Ray Profiles of the Hot Circumgalactic Medium. *ApJ* 936 (1), L15. doi:10.3847/2041-8213/ac8936. 2203.01356.
- CHIME/FRB Collaboration, Amiri M, Andersen BC, Bandura K, Berger S, Bhardwaj M, Boyce MM, Boyle PJ, Brar C, Breitman D, Cassanelli T, Chawla P, Chen T, Cliche JF, Cook A, Cubranic D, Curtin AP, Deng M, Dobbs M, Dong FA, Eadie G, Fandino M, Fonseca E, Gaensler BM, Giri U, Good DC, Halpern M, Hill AS, Hinshaw G, Josephy A, Kaczmarek JF, Kader Z, Kania JW, Kaspi VM, Landecker TL, Lang D, Leung C, Li D, Lin HH, Masui KW, McKinnen R, Mena-Parra J, Merryfield M, Meyers BW, Michilli D, Milutinovic N, Mirhosseini A, Münchmeyer M, Naidu A, Newburgh L, Ng C, Patel C, Pen UL, Petroff E, Pinsonneault-Marotte T, Pleunis Z, Rafiei-Ravandi M, Rahman M, Ransom SM, Renard A, Sanghavi P, Scholz P, Shaw JR, Shin K, Siegel SR, Sikora AE, Singh S, Smith KM, Stairs I, Tan CM, Tendulkar SP, Vanderlinde K, Wang H, Wulf D and Zwaniga AV (2021), Dec. The First CHIME/FRB Fast Radio Burst Catalog. *ApJS* 257 (2), 59. doi:10.3847/1538-4365/ac33ab. 2106.04352.
- Connor L, Ravi V, Catha M, Chen G, Faber JT, Lamb JW, Hallinan G, Harnach C, Hellbourg G, Hobbs R, Hodge D, Hodges M, Law C, Rasmussen P, Sayers J, Sharma K, Sherman MB, Shi J, Simard D, Somalwar J, Squillace R, Weinreb S, Woody DP, Yadlapalli N and Deep Synoptic Array Team (2023), Jun. Deep Synoptic Array Science: Two Fast Radio Burst Sources in Massive Galaxy Clusters. *ApJ* 949 (2), L26. doi:10.3847/2041-8213/acd3ea. 2302.14788.
- Connor L, Ravi V, Sharma K, Ocker SK, Faber J, Hallinan G, Harnach C, Hellbourg G, Hobbs R, Hodge D, Hodges M, Kosogorov N, Lamb J, Law C, Rasmussen P, Sherman M, Somalwar J, Weinreb S and Woody D (2024), Sep. A gas rich cosmic web revealed by partitioning the missing baryons. *arXiv e-prints*, arXiv:2409.16952doi:10.48550/arXiv.2409.16952. 2409.16952.
- Cordes JM (2004), Dec., NE2001: A New Model for the Galactic Electron Density and its Fluctuations, Clemens D, Shah R and Brainerd T, (Eds.), *Milky Way Surveys: The Structure and Evolution of our Galaxy*, Astronomical Society of the Pacific Conference Series, 317, pp. 211.
- Cordes JM and Chatterjee S (2019), Aug. Fast Radio Bursts: An Extragalactic Enigma. *ARA&A* 57: 417–465. doi:10.1146/annurev-astro-091918-104501. 1906.05878.
- Davé R, Cen R, Ostriker JP, Bryan GL, Hernquist L, Katz N, Weinberg DH, Norman ML and O'Shea B (2001), May. Baryons in the Warm-Hot Intergalactic Medium. *ApJ* 552 (2): 473–483. doi:10.1086/320548. astro-ph/0007217.
- Davé R, Anglés-Alcázar D, Narayanan D, Li Q, Rafieferantsoa MH and Appleby S (2019), Jun. SIMBA: Cosmological simulations with black hole growth and feedback. *MNRAS* 486 (2): 2827–2849. doi:10.1093/mnras/stz937. 1901.10203.
- de Graaff A, Cai YC, Heymans C and Peacock JA (2019), Apr. Probing the missing baryons with the Sunyaev-Zel'dovich effect from filaments. *A&A* 624, A48. doi:10.1051/0004-6361/201935159. 1709.10378.
- de Jong RS, Agertz O, Berbel AA, Aird J, Alexander DA, Amarsi A, Anders F, Andrae R, Ansarinejad B, Ansorge W and et al. (2019), Mar. 4MOST: Project overview and information for the First Call for Proposals. *The Messenger* 175: 3–11. doi:10.18727/0722-6691/5117. 1903.02464.
- Di Valentino E, Mena O, Pan S, Visinelli L, Yang W, Melchiorri A, Mota DF, Riess AG and Silk J (2021), Jul. In the realm of the Hubble tension—a review of solutions. *Classical and Quantum Gravity* 38 (15), 153001. doi:10.1088/1361-6382/ac086d. 2103.01183.
- Dolag K, Gaensler BM, Beck AM and Beck MC (2015), Aug. Constraints on the distribution and energetics of fast radio bursts using cosmological hydrodynamic simulations. *MNRAS* 451 (4): 4277–4289. doi:10.1093/mnras/stv1190. 1412.4829.
- Driessen LN, Barr ED, Buckley DAH, Caleb M, Chen H, Chen W, Gromadzki M, Jankowski F, Kraan-Korteweg RC, Palmerio J, Rajwade KM, Tremou E, Kramer M, Stappers BW, Vergani SD, Woudt PA, Bezuidenhout MC, Malenta M, Morello V, Sanidas S, Surnis MP and Fender RP (2024), Jan. FRB 202104051: a nearby Fast Radio Burst localized to sub-arcsecond precision with MeerKAT. *MNRAS* 527 (2): 3659–3673. doi:10.1093/mnras/stad3329. 2302.09787.
- Eckert D, Ettori S, Pointecouteau E, van der Burg RFJ and Loubser SI (2022), Jun. The gravitational field of X-COP galaxy clusters. *A&A* 662, A123. doi:10.1051/0004-6361/202142507. 2205.01110.
- Friedmann A (1922), Jan. Über die Krümmung des Raumes. *Zeitschrift für Physik* 10: 377–386. doi:10.1007/BF01332580.
- Fukugita M and Peebles PJE (2004), Dec. The Cosmic Energy Inventory. *ApJ* 616 (2): 643–668. doi:10.1086/425155. astro-ph/0406095.
- Fukugita M, Hogan CJ and Peebles PJE (1998), Aug. The Cosmic Baryon Budget. *ApJ* 503 (2): 518–530. doi:10.1086/306025. astro-ph/9712020.
- Ginzburg VL (1973), Dec. Possibility of Determining Intergalactic Gas Density by Radio Observations of Flares of Remote Sources. *Nature* 246 (5433): 415. doi:10.1038/246415a0.
- Glowacki M, Lee-Waddell K, Deller AT, Deg N, Gordon AC, Grundy JA, Marnoch L, Shen AX, Ryder SD, Shannon RM, Wong OI, Dénes H, Koribalski BS, Murugesan C, Rhee J, Westmeier T, Bhandari S, Bosma A, Holwerda BW and Prochaska JX (2023), May. WALLABY Pilot Survey: H I in the Host Galaxy of a Fast Radio Burst. *ApJ* 949 (1), 25. doi:10.3847/1538-4357/acc1e3. 2305.14863.

- Glowacki M, Bera A, Lee-Waddell K, Deller AT, Dial T, Gourdji K, Simha S, Caleb M, Marnoch L, Prochaska JX, Ryder SD, Shannon RM and Tejos N (2024), Feb. H I, FRB, What's Your z: The First FRB Host Galaxy Redshift from Radio Observations. *ApJ* 962 (1), L13. doi:10.3847/2041-8213/ad1f62. 2311.16808.
- Gordon AC, Fong WF, Kilpatrick CD, Eftekhar T, Leja J, Prochaska JX, Nugent AE, Bhandari S, Blanchard PK, Caleb M, Day CK, Deller AT, Dong Y, Glowacki M, Gourdji K, Mannings AG, Mahoney EK, Marnoch L, Miller AA, Paterson K, Rastinejad JC, Ryder SD, Sadler EM, Scott DR, Sears H, Shannon RM, Simha S, Stappers BW and Tejos N (2023), Sep. The Demographics, Stellar Populations, and Star Formation Histories of Fast Radio Burst Host Galaxies: Implications for the Progenitors. *ApJ* 954 (1), 80. doi:10.3847/1538-4357/ace5aa. 2302.05465.
- Hashimoto T, Goto T, On AYL, Lu TY, Santos DJD, Ho SCC, Wang TW, Kim SJ and Hsiao TYY (2020), Oct. Fast radio bursts to be detected with the Square Kilometre Array. *MNRAS* 497 (4): 4107–4116. doi:10.1093/mnras/staa2238. 2008.00007.
- Hashimoto T, Goto T, Lu TY, On AYL, Santos DJD, Kim SJ, Eser EK, Ho SCC, Hsiao TYY and Lin LYW (2021a), Apr. Revealing the cosmic reionization history with fast radio bursts in the era of Square Kilometre Array. *MNRAS* 502 (2): 2346–2355. doi:10.1093/mnras/stab186. 2101.08798.
- Hashimoto T, Goto T, Santos DJD, Ho SCC, Hsiao TYY, Wong YHV, On AYL, Kim SJ, Lu TY and Kilerci-Eser E (2021b), Dec. Upper limits on Einstein's weak equivalence principle placed by uncertainties of dispersion measures of fast radio bursts. *Phys. Rev. D* 104 (12), 124026. doi:10.1103/PhysRevD.104.124026. 2111.11447.
- Heimersheim S, Sartorio NS, Fialkov A and Lorimer DR (2022), Jul. What It Takes to Measure Reionization with Fast Radio Bursts. *ApJ* 933 (1), 57. doi:10.3847/1538-4357/ac70c9. 2107.14242.
- Hobbs G, Manchester RN, Dunning A, Jameson A, Roberts P, George D, Green JA, Tuthill J, Toomey L, Kaczmarek JF, Mader S, Marquarding M, Ahmed A, Amy SW, Bailes M, Beresford R, Bhat NDR, Bock DCJ, Bourne M, Bowen M, Brothers M, Cameron AD, Carretti E, Carter N, Castillo S, Chekkala R, Cheng W, Chung Y, Craig DA, Dai S, Dawson J, Dempsey J, Doherty P, Dong B, Edwards P, Ergesh T, Gao X, Han J, Hayman D, Indermuehle B, Jegannathan K, Johnston S, Kanoniuk H, Kesteven M, Kramer M, Leach M, McIntyre V, Moss V, Osłowski S, Phillips C, Pope N, Preisig B, Price D, Reeves K, Reilly L, Reynolds J, Robishaw T, Roush P, Ruckley T, Sadler E, Sarkissian J, Severs S, Shannon R, Smart K, Smith M, Smith S, Sobey C, Staveley-Smith L, Tzioumis A, van Straten W, Wang N, Wen L and Whiting M (2020), Apr. An ultra-wide bandwidth (704 to 4 032 MHz) receiver for the Parkes radio telescope. *PASA* 37, e012. doi:10.1017/pasa.2020.2. 1911.00656.
- Hoffmann J, James CW, Glowacki M, Prochaska JX, Gordon AC, Deller AT, Shannon RM and Ryder SD (2024), Aug. Modelling DSA, FAST and CRAFT surveys in a z-DM analysis and constraining a minimum FRB energy. *arXiv e-prints*, arXiv:2408.04878doi:10.48550/arXiv.2408.04878. 2408.04878.
- Huang Y, Simha S, Khrykin I, Lee KG, Prochaska JX, Tejos N, Bannister K, Barrios J, Chisholm J, Cooke J, Deller A, Glowacki M, Marnoch L, Shannon R and Zhang J (2024), Aug. FRB Line-of-sight Ionization Measurement From Lightcone AAOmega Mapping Survey: the First Data Release. *arXiv e-prints*, arXiv:2408.12864doi:10.48550/arXiv.2408.12864. 2408.12864.
- Hubble E (1929), Mar. A Relation between Distance and Radial Velocity among Extra-Galactic Nebulae. *Proceedings of the National Academy of Science* 15 (3): 168–173. doi:10.1073/pnas.15.3.168.
- Inoue S (2004), Mar. Probing the cosmic reionization history and local environment of gamma-ray bursts through radio dispersion. *MNRAS* 348 (3): 999–1008. doi:10.1111/j.1365-2966.2004.07359.x. astro-ph/0309364.
- Ioka K (2003), Dec. The Cosmic Dispersion Measure from Gamma-Ray Burst Afterglows: Probing the Reionization History and the Burst Environment. *ApJ* 598 (2): L79–L82. doi:10.1086/380598. astro-ph/0309200.
- James CW, Ghosh EM, Prochaska JX, Bannister KW, Bhandari S, Day CK, Deller AT, Glowacki M, Gordon AC, Heintz KE, Marnoch L, Ryder SD, Scott DR, Shannon RM and Tejos N (2022), Nov. A measurement of Hubble's Constant using Fast Radio Bursts. *MNRAS* 516 (4): 4862–4881. doi:10.1093/mnras/stac2524. 2208.00819.
- Jaroszynski M (2019), Apr. Fast radio bursts and cosmological tests. *MNRAS* 484 (2): 1637–1644. doi:10.1093/mnras/sty3529. 1812.11936.
- Jiang P, Chen R, Gan H, Sun J, Zhu B, Li H, Zhu W, Wu J, Chen X, Zhang H and An T (2024), Jan. The FAST Core Array. *Astronomical Techniques and Instruments* 1 (2): 84–94. doi:10.61977/ati2024012. 2408.12826.
- Kafle PR, Sharma S, Lewis GF and Bland-Hawthorn J (2014), Oct. On the Shoulders of Giants: Properties of the Stellar Halo and the Milky Way Mass Distribution. *ApJ* 794 (1), 59. doi:10.1088/0004-637X/794/1/59. 1408.1787.
- Kalita S, Bhatporia S and Weltman A (2024), Oct. Fast Radio Bursts as probes of the late-time universe: a new insight on the Hubble tension. *arXiv e-prints*, arXiv:2410.01974doi:10.48550/arXiv.2410.01974. 2410.01974.
- Khrykin IS, Ata M, Lee KG, Simha S, Huang Y, Prochaska JX, Tejos N, Bannister KW, Cooke J, Day CK, Deller A, Glowacki M, Gordon AC, James CW, Marnoch L, Shannon RM, Zhang J and Bernalles-Cortes L (2024a), Oct. FLIMFLAM DR1: The First Constraints on the Cosmic Baryon Distribution from Eight Fast Radio Burst Sight Lines. *ApJ* 973 (2), 151. doi:10.3847/1538-4357/ad6567. 2402.00505.
- Khrykin IS, Sorini D, Lee KG and Davé R (2024b), Mar. The cosmic baryon partition between the IGM and CGM in the SIMBA simulations. *MNRAS* 529 (1): 537–549. doi:10.1093/mnras/stae525. 2310.01496.
- Kovacs TO, Mao SA, Basu A, Ma YK, Pakmor R, Spitler LG and Walker CRH (2024), Oct. Dispersion and rotation measures from fast radio burst (FRB) host galaxies based on the TNG50 simulation. *A&A* 690, A47. doi:10.1051/0004-6361/202347459. 2407.16748.
- Lanman AE, Andrew S, Lazda M, Shah V, Amiri M, Balasubramanian A, Bandura K, Boyle PJ, Brar C, Carlson M, Cliche JF, Gusinskaia N, Hendricksen IT, Kaczmarek JF, Landecker T, Leung C, Mckinven R, Mena-Parra J, Milutinovic N, Nimmo K, Pearlman AB, Renard A, Rahman M, Shaw JR, Siegel SR, Smegal RJ, Cassanelli T, Chatterjee S, Curtin AP, Dobbs M, Dong FA, Halpern M, Hopkins H, Kaspi VM, Khairy K, Masui KW, Meyers BW, Michilli D, Petroff E, Pinsonneault-Marotte T, Pleunis Z, Rafiei-Ravandi M, Shin K, Smith K, Vanderlinde K and Zegmott TJ (2024), Aug. CHIME/FRB Outriggers: KKO Station System and Commissioning Results. *AJ* 168 (2), 87. doi:10.3847/1538-3881/ad5838. 2402.07898.
- Law CJ, Sharma K, Ravi V, Chen G, Catha M, Connor L, Faber JT, Hallinan G, Harnach C, Hellbourg G, Hobbs R, Hodge D, Hodges M, Lamb JW, Rasmussen P, Sherman MB, Shi J, Simard D, Squillace R, Weinreb S, Woody DP and Yurk NY (2024), May. Deep Synoptic Array Science: First FRB and Host Galaxy Catalog. *ApJ* 967 (1), 29. doi:10.3847/1538-4357/ad3736. 2307.03344.
- Lee KG, Ata M, Khrykin IS, Huang Y, Prochaska JX, Cooke J, Zhang J and Batten A (2022), Mar. Constraining the Cosmic Baryon Distribution with Fast Radio Burst Foreground Mapping. *ApJ* 928 (1), 9. doi:10.3847/1538-4357/ac4f62. 2109.00386.
- Lee KG, Khrykin IS, Simha S, Ata M, Huang Y, Prochaska JX, Tejos N, Cooke J, Nagamine K and Zhang J (2023), Sep. The FRB 20190520B Sight Line Intersects Foreground Galaxy Clusters. *ApJ* 954 (1), L7. doi:10.3847/2041-8213/acefb5. 2306.05403.
- Lin HH, Lin Ky, Li CT, Tseng YH, Jiang H, Wang JH, Cheng JC, Pen UL, Chen MT, Chen P, Chen Y, Goto T, Hashimoto T, Hwang YJ, King SK, Kubo D, Kuo CY, Mills A, Nam J, Oshiro P, Shen CS, Tseng HC, Wang SH, Wu VFS, Bower G, Chang SH, Chen PA, Chen YC, Chiang YK, Fedynitch A, Gusinskaia N, Ho SCC, Hsiao TYY, Hu CP, Huang YD, Jáuregui García JM, Kim SJ, Kuo CY, Ling DFJ, On AYL, Peterson JB, R. Raquel BJ, Su SC, Uno Y, Wu KW, Yamasaki S and Zhu HM (2022), Sep. BURSTT: Bustling Universe Radio Survey Telescope in Taiwan. *PASP* 134 (1039), 094106. doi:10.1088/1538-3873/ac8f71. 2206.08983.
- Lorimer DR, Bailes M, McLaughlin MA, Narkevic DJ and Crawford F (2007), Nov. A Bright Millisecond Radio Burst of Extragalactic Origin. *Science* 318 (5851): 777. doi:10.1126/science.1147532. 0709.4301.

- Lorimer DR, McLaughlin MA and Bailes M (2024), Jun. The discovery and significance of fast radio bursts. *Ap&SS* 369 (6), 59. doi:10.1007/s10509-024-04322-6. 2405.19106.
- Luo R, Ekers RD, Hobbs G, Dunning A, James CW, Lower ME, Gupta V, Zic A, Sokolowski M, Phillips C, Deller AT and Staveley-Smith L (2024), May. A Fast Radio Burst monitor with a Compact All-Sky Phased Array (CASPA). *arXiv e-prints*, arXiv:2405.07439doi:10.48550/arXiv.2405.07439. 2405.07439.
- Macquart JP, Prochaska JX, McQuinn M, Bannister KW, Bhandari S, Day CK, Deller AT, Ekers RD, James CW, Marnoch L, Ostrowski S, Phillips C, Ryder SD, Scott DR, Shannon RM and Tejos N (2020), May. A census of baryons in the Universe from localized fast radio bursts. *Nature* 581 (7809): 391–395. doi:10.1038/s41586-020-2300-2. 2005.13161.
- Maller AH and Bullock JS (2004), Dec. Multiphase galaxy formation: high-velocity clouds and the missing baryon problem. *MNRAS* 355 (3): 694–712. doi:10.1111/j.1365-2966.2004.08349.x. astro-ph/0406632.
- Mannings AG, Fong WF, Simha S, Prochaska JX, Rafelski M, Kilpatrick CD, Tejos N, Heintz KE, Bannister KW, Bhandari S, Day CK, Deller AT, Ryder SD, Shannon RM and Tendulkar SP (2021), Aug. A High-resolution View of Fast Radio Burst Host Environments. *ApJ* 917 (2), 75. doi:10.3847/1538-4357/abff56. 2012.11617.
- Mannings AG, Pakmor R, Prochaska JX, van de Voort F, Simha S, Shannon RM, Tejos N, Deller A and Rafelski M (2023), Sep. Fast Radio Bursts as Probes of Magnetic Fields in Galaxies at $z \lesssim 0.5$. *ApJ* 954 (2), 179. doi:10.3847/1538-4357/ace7bb. 2209.15113.
- Mantz AB, Allen SW, Morris RG, Rapetti DA, Applegate DE, Kelly PL, von der Linden A and Schmidt RW (2014), May. Cosmology and astrophysics from relaxed galaxy clusters - II. Cosmological constraints. *MNRAS* 440 (3): 2077–2098. doi:10.1093/mnras/stu368. 1402.6212.
- Martizzi D, Quataert E, Faucher-Giguère CA and Fielding D (2019), Feb. Simulations of jet heating in galaxy clusters: successes and challenges. *MNRAS* 483 (2): 2465–2486. doi:10.1093/mnras/sty3273. 1805.06461.
- McLaughlin MA and Cordes JM (2003), Oct. Searches for Giant Pulses from Extragalactic Pulsars. *ApJ* 596 (2): 982–996. doi:10.1086/378232. astro-ph/0304365.
- McQuinn M (2014), Jan. Locating the “Missing” Baryons with Extragalactic Dispersion Measure Estimates. *ApJ* 780 (2), L33. doi:10.1088/2041-8205/780/2/L33. 1309.4451.
- Medlock I, Nagai D, Singh P, Oppenheimer B, Anglés-Alcázar D and Villaescusa-Navarro F (2024), May. Probing the Circumgalactic Medium with Fast Radio Bursts: Insights from CAMELS. *ApJ* 967 (1), 32. doi:10.3847/1538-4357/ad3070. 2403.02313.
- Neeleman M, Prochaska JX, Ribaud J, Lehner N, Howk JC, Rafelski M and Kanekar N (2016), Feb. The H I Content of the Universe Over the Past 10 GYRS. *ApJ* 818 (2), 113. doi:10.3847/0004-637X/818/2/113. 1601.01691.
- Nicastro F, Kaastra J, Krongold Y, Borgani S, Branchini E, Cen R, Dadina M, Danforth CW, Elvis M, Fiore F, Gupta A, Mathur S, Mayya D, Paerels F, Piro L, Rosa-Gonzalez D, Schaye J, Shull JM, Torres-Zafra J, Wijers N and Zappacosta L (2018), Jun. Observations of the missing baryons in the warm-hot intergalactic medium. *Nature* 558 (7710): 406–409. doi:10.1038/s41586-018-0204-1. 1806.08395.
- Niu CH, Aggarwal K, Li D, Zhang X, Chatterjee S, Tsai CW, Yu W, Law CJ, Burke-Spolaor S, Cordes JM, Zhang YK, Ocker SK, Yao JM, Wang P, Feng Y, Niino Y, Bochenek C, Cruces M, Connor L, Jiang JA, Dai S, Luo R, Li GD, Miao CC, Niu JR, Anna-Thomas R, Sydnor J, Stern D, Wang WY, Yuan M, Yue YL, Zhou DJ, Yan Z, Zhu WW and Zhang B (2022), Jun. A repeating fast radio burst associated with a persistent radio source. *Nature* 606 (7916): 873–877. doi:10.1038/s41586-022-04755-5. 2110.07418.
- Ocker SK, Cordes JM, Chatterjee S, Niu CH, Li D, McKee JW, Law CJ, Tsai CW, Anna-Thomas R, Yao JM and Cruces M (2022), Jun. The Large Dispersion and Scattering of FRB 20190520B Are Dominated by the Host Galaxy. *ApJ* 931 (2), 87. doi:10.3847/1538-4357/ac6504. 2202.13458.
- Orr ME, Burkhart B, Lu W, Ponnada SB and Hummels CB (2024), Sep. Objects May Be Closer than They Appear: Significant Host Galaxy Dispersion Measures of Fast Radio Bursts in Zoom-in Simulations. *ApJ* 972 (2), L26. doi:10.3847/2041-8213/ad725b. 2406.03523.
- Planck Collaboration, Aghanim N, Akrami Y, Ashdown M, Aumont J, Baccigalupi C, Ballardini M, Banday AJ, Barreiro RB, Bartolo N, Basak S, Battye R, Benabed K, Bernard JP, Bersanelli M, Bielewicz P, Bock JJ, Bond JR, Borrill J, Bouchet FR, Boulanger F, Bucher M, Burigana C, Butler RC, Calabrese E, Cardoso JF, Carron J, Challinor A, Chiang HC, Chluba J, Colombo LPL, Combet C, Contreras D, Crill BP, Cuttaia F, de Bernardis P, de Zotti G, Delabrouille J, Delouis JM, Di Valentino E, Diego JM, Doré O, Douspis M, Ducout A, Dupac X, Dusini S, Efstathiou G, Elsner F, Enßlin TA, Eriksen HK, Fantaye Y, Farhang M, Fergusson J, Fernandez-Cobos R, Finelli F, Forastieri F, Frailis M, Fraisse AA, Franceschi E, Frolov A, Galeotta S, Galli S, Ganga K, Génova-Santos RT, Gerbino M, Ghosh T, González-Nuevo J, Górski KM, Gratton S, Gruppiso A, Gudmundsson JE, Hamann J, Handley W, Hansen FK, Herranz D, Hildebrandt SR, Hivon E, Huang Z, Jaffe AH, Jones WC, Karakci A, Keihänen E, Keskitalo R, Kiiveri K, Kim J, Kisner TS, Knox L, Krachmalnicoff N, Kunz M, Kurki-Suonio H, Lagache G, Lamarre JM, Lasenby A, Lattanzi M, Lawrence CR, Le Jeune M, Lemos P, Lesgourgues J, Levrier F, Lewis A, Liguori M, Lilje PB, Lilley M, Lindholm V, López-Cañiego M, Lubin PM, Ma YZ, Macías-Pérez JF, Maggio G, Maino D, Mandolesi N, Mangilli A, Marcos-Caballero A, Maris M, Martin PG, Martinelli M, Martínez-González E, Matarrese S, Mauri N, McEwen JD, Meinhold PR, Melchiorri A, Mennella A, Migliaccio M, Millea M, Mitra S, Miville-Deschênes MA, Molinari D, Montier L, Morgante G, Moss A, Natoli P, Nørgaard-Nielsen HU, Pagano L, Paoletti D, Partridge B, Patanchon G, Peiris HV, Perrotta F, Pettorino V, Piacentini F, Polastri L, Polenta G, Puget JL, Rachen JP, Reinecke M, Remazeilles M, Renzi A, Rocha G, Rosset C, Roudier G, Rubiño-Martín JA, Ruiz-Granados B, Salvati L, Sandri M, Savelainen M, Scott D, Shellard EPS, Sirignano C, Sirri G, Spencer LD, Sunyaev R, Suur-Uski AS, Tauber JA, Tavagnacco D, Tenti M, Toffolatti L, Tomasi M, Trombetti T, Valenziano L, Valiviita J, Van Tent B, Vibert L, Vielva P, Villa F, Vittorio N, Wandelt BD, Wehus IK, White M, White SDM, Zacchei A and Zonca A (2020), Sep. Planck 2018 results. VI. Cosmological parameters. *A&A* 641, A6. doi:10.1051/0004-6361/201833910. 1807.06209.
- Pol N, Lam MT, McLaughlin MA, Lazio TJW and Cordes JM (2019), Dec. Estimates of Fast Radio Burst Dispersion Measures from Cosmological Simulations. *ApJ* 886 (2), 135. doi:10.3847/1538-4357/ab4c2f. 1903.07630.
- Prochaska JX and Zheng Y (2019), May. Probing Galactic haloes with fast radio bursts. *MNRAS* 485 (1): 648–665. doi:10.1093/mnras/stz261. 1901.11051.
- Prochaska JX, Macquart JP, McQuinn M, Simha S, Shannon RM, Day CK, Marnoch L, Ryder S, Deller A, Bannister KW, Bhandari S, Bordoloi R, Bunton J, Cho H, Flynn C, Mahony EK, Phillips C, Qiu H and Tejos N (2019), Oct. The low density and magnetization of a massive galaxy halo exposed by a fast radio burst. *Science* 366 (6462): 231–234. doi:10.1126/science.aay0073. 1909.11681.
- Rafiei-Ravandi M, Smith KM, Li D, Masui KW, Josephy A, Dobbs M, Lang D, Bhardwaj M, Patel C, Bandura K, Berger S, Boyle PJ, Brar C, Breitman D, Cassanelli T, Chawla P, Adam Dong F, Fonseca E, Gaensler BM, Giri U, Good DC, Halpern M, Kaczmarek J, Kaspi VM, Leung C, Lin HH, Mena-Parra J, Meyers BW, Michilli D, Münchmeyer M, Ng C, Petroff E, Pleunis Z, Rahman M, Sanghavi P, Scholz P, Shin K, Stairs IH, Tendulkar SP, Vanderlinde K and Zwaniga A (2021), Nov. CHIME/FRB Catalog 1 Results: Statistical Cross-correlations with Large-scale Structure. *ApJ* 922 (1), 42. doi:10.3847/1538-4357/ac1dab. 2106.04354.
- Rasheed B, Bahcall N and Bode P (2011), Mar. Searching for the missing baryons in clusters. *Proceedings of the National Academy of Science* 108 (9): 3487–3492. doi:10.1073/pnas.1009878108. 1007.1980.
- Ravi V (2019), Feb. Measuring the Circumgalactic and Intergalactic Baryon Contents with Fast Radio Bursts. *ApJ* 872 (1), 88. doi:10.3847/1538-4357/aaf30. 1804.07291.
- Ravi V, Shannon RM, Bailes M, Bannister K, Bhandari S, Bhat NDR, Burke-Spolaor S, Caleb M, Flynn C, Jameson A, Johnston S, Keane EF, Kerr M, Tiburzi C, Tuntsov AV and Vedantham HK (2016), Dec. The magnetic field and turbulence of the cosmic web measured using a

- brilliant fast radio burst. *Science* 354 (6317): 1249–1252. doi:10.1126/science.aaf6807. 1611.05758.
- Ravi V, Catha M, Chen G, Connor L, Cordes JM, Faber JT, Lamb JW, Hallinan G, Harnach C, Hellbourg G, Hobbs R, Hodge D, Hodges M, Law C, Rasmussen P, Sharma K, Sherman MB, Shi J, Simard D, Somalwar JJ, Squillace R, Weinreb S, Woody DP and Yadlapalli N (2023), Jan. Deep Synoptic Array science: a 50 Mpc fast radio burst constrains the mass of the Milky Way circumgalactic medium. *arXiv e-prints*, arXiv:2301.01000doi:10.48550/arXiv.2301.01000. 2301.01000.
- Riess AG, Yuan W, Macri LM, Scolnic D, Brout D, Casertano S, Jones DO, Murakami Y, Anand GS, Breuval L, Brink TG, Filippenko AV, Hoffmann S, Jha SW, D'Arcy Kenworthy W, Mackenty J, Stahl BE and Zheng W (2022), Jul. A Comprehensive Measurement of the Local Value of the Hubble Constant with $1 \text{ km s}^{-1} \text{ Mpc}^{-1}$ Uncertainty from the Hubble Space Telescope and the SH0ES Team. *ApJ* 934 (1), L7. doi:10.3847/2041-8213/ac5c5b. 2112.04510.
- Ryder SD, Bannister KW, Bhandari S, Deller AT, Ekers RD, Glowacki M, Gordon AC, Gourdji K, James CW, Kilpatrick CD, Lu W, Marnoch L, Moss VA, Prochaska JX, Qiu H, Sadler EM, Simha S, Sammons MW, Scott DR, Tejos N and Shannon RM (2023), Oct. A luminous fast radio burst that probes the Universe at redshift 1. *Science* 382 (6668): 294–299. doi:10.1126/science.adf2678. 2210.04680.
- Schaye J, Kugel R, Schaller M, Helly JC, Braspennig J, Elbers W, McCarthy IG, van Daalen MP, Vandenbroucke B, Frenk CS, Kwan J, Salcido J, Bahé YM, Borrow J, Chaikin E, Hahn O, Huško F, Jenkins A, Lacey CG and Nobels FSJ (2023), Dec. The FLAMINGO project: cosmological hydrodynamical simulations for large-scale structure and galaxy cluster surveys. *MNRAS* 526 (4): 4978–5020. doi:10.1093/mnras/stad2419. 2306.04024.
- Scott DR, Cho H, Day CK, Deller AT, Glowacki M, Gourdji K, Bannister KW, Bera A, Bhandari S, James CW and Shannon RM (2023), Jul. CELEBI: The CRAFT Effortless Localisation and Enhanced Burst Inspection pipeline. *Astronomy and Computing* 44, 100724. doi:10.1016/j.ascom.2023.100724. 2301.13484.
- Shannon RM, Bannister KW, Bera A, Bhandari S, Day CK, Deller AT, Dial T, Dobie D, Ekers RD, Fong Wf, Glowacki M, Gordon AC, Gourdji K, Jaini A, James CW, Kumar P, Mahony EK, Marnoch L, Muller AR, Prochaska JX, Qiu H, Ryder SD, Sadler EM, Scott DR, Tejos N, Uttarkar PA and Wang Y (2024), Aug. The Commensal Real-time ASKAP Fast Transient incoherent-sum survey. *arXiv e-prints*, arXiv:2408.02083doi:10.48550/arXiv.2408.02083. 2408.02083.
- Shapiro II (1964), Dec. Fourth Test of General Relativity. *Phys. Rev. Lett.* 13 (26): 789–791. doi:10.1103/PhysRevLett.13.789.
- Sharma K, Ravi V, Connor L, Law C, Ocker SK, Sherman M, Kosogorov N, Faber J, Hallinan G, Harnach C, Hellbourg G, Hobbs R, Hodge D, Hodges M, Lamb J, Rasmussen P, Somalwar J, Weinreb S, Woody D, Leja J, Anand S, Kashyap Das K, Qin YJ, Rose S, Dong DZ, Miller J and Yao Y (2024), Sep. Preferential Occurrence of Fast Radio Bursts in Massive Star-Forming Galaxies. *arXiv e-prints*, arXiv:2409.16964doi:10.48550/arXiv.2409.16964. 2409.16964.
- Sherman MB, Connor L, Ravi V, Law C, Chen G, Catha M, Faber JT, Hallinan G, Harnach C, Hellbourg G, Hobbs R, Hodge D, Hodges M, Lamb JW, Rasmussen P, Sharma K, Shi J, Simard D, Somalwar J, Squillace R, Weinreb S, Woody DP, Yadlapalli N and The Deep Synoptic Array team (2024), Apr. Deep Synoptic Array Science: Polarimetry of 25 New Fast Radio Bursts Provides Insights into Their Origins. *ApJ* 964 (2), 131. doi:10.3847/1538-4357/ad275e. 2308.06813.
- Shin K, Leung C, Simha S, Andersen BC, Fonseca E, Nimmo K, Bhardwaj M, Brar C, Chatterjee S, Cook AM, Gaensler BM, Joseph RC, Jow D, Kaczmarek J, Kahinga L, Kaspi VM, Kharel B, Lanman AE, Lazda M, Main RA, Mas-Ribas L, Masui KW, Mena-Parra J, Michilli D, Pandhi A, Shivraj Patil S, Pearlman AB, Pleunis Z, Prochaska JX, Rafiei-Ravandi M, Sammons MW, Sand KR, Smith K and Stairs I (2024), Oct. Investigating the sightline of a highly scattered FRB through a filamentary structure in the local Universe. *arXiv e-prints*, arXiv:2410.07307doi:10.48550/arXiv.2410.07307. 2410.07307.
- Simha S, Burchett JN, Prochaska JX, Chittidi JS, Elek O, Tejos N, Jorgenson R, Bannister KW, Bhandari S, Day CK, Deller AT, Forbes AG, Macquart JP, Ryder SD and Shannon RM (2020), Oct. Disentangling the Cosmic Web toward FRB 190608. *ApJ* 901 (2), 134. doi:10.3847/1538-4357/abafc3. 2005.13157.
- Simha S, Lee KG, Prochaska JX, Khrykin IS, Huang Y, Tejos N, Marnoch L, Ata M, Bernales L, Bhandari S, Cooke J, Deller AT, Ryder SD and Zhang J (2023), Sep. Searching for the Sources of Excess Extragalactic Dispersion of FRBs. *ApJ* 954 (1), 71. doi:10.3847/1538-4357/ace324. 2303.07387.
- Singh P, Lau ET, Faerman Y, Stern J and Nagai D (2024), Aug. Comparison of models for the warm-hot circumgalactic medium around Milky Way-like galaxies. *MNRAS* 532 (3): 3222–3235. doi:10.1093/mnras/stae1695. 2407.06555.
- Sorini D, Davé R, Cui W and Appleby S (2022), Oct. How baryons affect haloes and large-scale structure: a unified picture from the SIMBA simulation. *MNRAS* 516 (1): 883–906. doi:10.1093/mnras/stac2214. 2111.13708.
- Spitler LG, Cordes JM, Hessels JWT, Lorimer DR, McLaughlin MA, Chatterjee S, Crawford F, Deneva JS, Kaspi VM, Wharton RS, Allen B, Bogdanov S, Brazier A, Camilo F, Freire PCC, Jenet FA, Karako-Argaman C, Knispel B, Lazarus P, Lee KJ, van Leeuwen J, Lynch R, Ransom SM, Scholz P, Siemens X, Stairs IH, Stovall K, Swiggum JK, Venkataraman A, Zhu WW, Aulbert C and Fehrmann H (2014), Aug. Fast Radio Burst Discovered in the Arecibo Pulsar ALFA Survey. *ApJ* 790 (2), 101. doi:10.1088/0004-637X/790/2/101. 1404.2934.
- Stern J, Fielding D, Faucher-Giguère CA and Quataert E (2019), Sep. Cooling flow solutions for the circumgalactic medium. *MNRAS* 488 (2): 2549–2572. doi:10.1093/mnras/stz1859. 1906.07737.
- Takahashi R, Ioka K, Mori A and Funahashi K (2021), Apr. Statistical modelling of the cosmological dispersion measure. *MNRAS* 502 (2): 2615–2629. doi:10.1093/mnras/stab170. 2010.01560.
- Thornton D, Stappers B, Bailes M, Barsdell B, Bates S, Bhat NDR, Burgay M, Burke-Spolaor S, Champion DJ, Coster P, D'Amico N, Jameson A, Johnston S, Keith M, Kramer M, Levin L, Milia S, Ng C, Possenti A and van Straten W (2013), Jul. A Population of Fast Radio Bursts at Cosmological Distances. *Science* 341 (6141): 53–56. doi:10.1126/science.1236789. 1307.1628.
- Tumlinson J, Peebles MS and Werk JK (2017), Aug. The Circumgalactic Medium. *ARA&A* 55 (1): 389–432. doi:10.1146/annurev-astro-091916-055240. 1709.09180.
- Villaescusa-Navarro F, Anglés-Alcázar D, Genel S, Spergel DN, Somerville RS, Dave R, Pillepich A, Hernquist L, Nelson D, Torrey P, Narayanan D, Li Y, Philcox O, La Torre V, Maria Delgado A, Ho S, Hassan S, Burkhardt B, Wadekar D, Battaglia N, Contardo G and Bryan GL (2021), Jul. The CAMELS Project: Cosmology and Astrophysics with Machine-learning Simulations. *ApJ* 915 (1), 71. doi:10.3847/1538-4357/abf7ba. 2010.00619.
- Walker CRH, Spitler LG, Ma YZ, Cheng C, Artale MC and Hummels CB (2024), Mar. The dispersion measure contributions of the cosmic web. *A&A* 683, A71. doi:10.1051/0004-6361/202347139. 2309.08268.
- Werk JK, Prochaska JX, Tumlinson J, Peebles MS, Tripp TM, Fox AJ, Lehner N, Thom C, O'Meara JM, Ford AB, Bordoloi R, Katz N, Tejos N, Oppenheimer BD, Davé R and Weinberg DH (2014), Sep. The COS-Halos Survey: Physical Conditions and Baryonic Mass in the Low-redshift Circumgalactic Medium. *ApJ* 792 (1), 8. doi:10.1088/0004-637X/792/1/8. 1403.0947.
- Wirtz C (1922), Apr. Einiges zur Statistik der Radialbewegungen von Spiralnebeln und Kugelsternhaufen. *Astronomische Nachrichten* 215: 349. doi:10.1002/asna.19212151703.
- Wu XF, Zhang SB, Gao H, Wei JJ, Zou YC, Lei WH, Zhang B, Dai ZG and Mészáros P (2016), May. Constraints on the Photon Mass with Fast Radio Bursts. *ApJ* 822 (1), L15. doi:10.3847/2041-8205/822/1/L15. 1602.07835.

- Wucknitz O, Spitler LG and Pen UL (2021), Jan. Cosmology with gravitationally lensed repeating fast radio bursts. *A&A* 645, A44. doi:10.1051/0004-6361/202038248. 2004.11643.
- Yao JM, Manchester RN and Wang N (2017), Jan. A New Electron-density Model for Estimation of Pulsar and FRB Distances. *ApJ* 835 (1), 29. doi:10.3847/1538-4357/835/1/29. 1610.09448.
- Zhang GQ, Yu H, He JH and Wang FY (2020), Sep. Dispersion Measures of Fast Radio Burst Host Galaxies Derived from IllustrisTNG Simulation. *ApJ* 900 (2), 170. doi:10.3847/1538-4357/abaa4a. 2007.13935.
- Zhang JG, Zhao ZW, Li Y, Zhang JF, Li D and Zhang X (2023), Dec. Cosmology with fast radio bursts in the era of SKA. *Science China Physics, Mechanics, and Astronomy* 66 (12), 120412. doi:10.1007/s11433-023-2212-9. 2307.01605.
- Zheng Z, Ofek EO, Kulkarni SR, Neill JD and Juric M (2014), Dec. Probing the Intergalactic Medium with Fast Radio Bursts. *ApJ* 797 (1), 71. doi:10.1088/0004-637X/797/1/71. 1409.3244.
- Zhu W and Feng LL (2021), Jan. The Dispersion Measure and Scattering of Fast Radio Bursts: Contributions from the Intergalactic Medium, Foreground Halos, and Hosts. *ApJ* 906 (2), 95. doi:10.3847/1538-4357/abcb90. 2011.08519.